Zero sound and first sound in thin arbitrarily polarized Fermi-liquid films

David Z. Li,* R. H. Anderson,† and M. D. Miller‡
Department of Physics and Astronomy, Washington State University, Pullman, Washington 99164-2814, USA
(Received 20 December 2012; published 29 March 2013)

We study the propagation and attenuation of zero sound and first sound in thin, arbitrarily polarized Fermi-liquid films. Following Khalatnikov and Abrikosov, we solve Landau's linearized kinetic equation in the relaxation-time approximation for a complex speed of sound. Analytic solutions are obtained in the hydrodynamic and ballistic limits for arbitrary polarization. By solving the collision integral in two dimensions, we find the well-known result that quasiparticle-quasiparticle collisions contribute to the collision frequencies $1/\tau_\sigma$, with a low-temperature term proportional to $T^2 \ln(T_{F\sigma}/T)$, where $\sigma = \uparrow, \downarrow$ is the spin state. If the films are adsorbed to a dynamic substrate, we find additional possible contributions to the collision frequency that come from quasiparticle-phonon interactions. We show, however, that for ^{3}He thin films, the mismatch between possible maximum values of the Fermi velocity and the substrate speed of sound freezes this contribution out at usual experimental temperatures. Thus, we can conclude that zero sound propagates at absolute zero in this type of adsorbed Fermi-liquid film. By utilizing previous results for the Landau parameters of an arbitrarily polarized ^{3}He film, we compute numerical solutions for the sound speeds and attenuation in the hydrodynamic and ballistic regimes, thereby studying the transition from first sound to zero sound as a function of temperature.

DOI: 10.1103/PhysRevB.87.104519 PACS number(s): 67.30.ep, 67.30.hr

I. INTRODUCTION

Fermi-liquid theory, developed by Landau[1] in the mid 1950s, showed that the low-temperature collective excitations and thermodynamic properties of *normal* many-fermion systems could be encoded in a few parameters, the Landau parameters, and that these parameters were related to a certain limiting value of the microscopic scattering function.[2] Thin films of normal ^{3}He have been studied experimentally for many years as prototypical two-dimensional Fermi liquids.[3–8] In a recent series of papers[9–11] [Li, Anderson, and Miller (LAM)], we have utilized a perturbation-theory-based approach to study the properties of thin, arbitrarily polarized Fermi-liquid films. Perturbation theory was applied to the low-density Fermi gas in three dimensions by Khalatnikov and Abrikosov (KA).[12] More recently, Engelbrecht, Randeria, and Zhang[13] (ERZ) obtained an analytic solution for the s-wave contribution to the low-density, unpolarized Fermi gas in *two* dimensions. As stressed by ERZ, the key to obtaining analytic results in two dimensions is the constant density of states. In LAM, the perturbation-theory approach of ERZ was generalized to include p-wave T-matrix interactions. The Landau parameters were calculated exactly and analytically to quadratic order in the s- and p-wave interaction parameters. These Landau parameters can thus be used at arbitrary values of the polarization. A rigorous discussion of the generalization of Fermi-liquid theory to polarized systems was given by Bedell and Quader.[14]

In LAM, the Fermi-liquid expressions for thermodynamic quantities and collective excitations were obtained for arbitrary polarization. The Landau parameter values can be easily obtained once the the s- and p-wave interaction components have been determined. Density-dependent values for these T-matrix components were obtained by fitting existing experimental data for the effective mass and the spin susceptibility. This was done for two systems: second-layer ^{3}He films on a graphite substrate[5,6] and also for submonolayer ^{3}He adsorbed in thin ^{4}He superfluid films.[15] We were then able to calculate predicted values as a function of density for the effective mass and spin susceptibility at finite polarization, and for the compressibility and zero sound at all polarizations. In this paper, we extend the work on the collective excitations to examine propagation and attenuation for zero sound and first sound at low temperatures. To this end, in Sec. II we shall closely follow the approach of KA to derive expressions for the speed of sound and the attenuation in terms of the Landau parameters and the collision frequency. In Sec. III, we calculate the low-temperature behavior of the collision integral in the relaxation-time approximation. One contribution to the relaxation time comes from quasiparticle-quasiparticle collisions, the same as in three dimensions.[16] For adsorbed films, there is also the possibility that significant contribution to the total collision frequency can come from quasiparticle-phonon collisions, where the phonon in this case is an excitation in the adsorbing substrate. In Sec. IV, we study the transition from first sound to zero sound in a second-layer film of ^{3}He adsorbed to a graphite substrate as we lower the temperature by numerically solving the general polarization-dependent kinetic equation combined with our results for the collision frequency. Section V is the conclusion.

II. SOUND SPEED AND ATTENUATION

We examine a system of $N = N_\uparrow + N_\downarrow$, spin-$\frac{1}{2}$ fermions in a box of area L^2. The particles have bare mass m and interact with a two-body potential $V(r)$ that is assumed to depend only on the scalar distance between the particles. The particles fill two Fermi seas up to Fermi momenta $k_\uparrow$ and $k_\downarrow$, and we introduce the convention that the spin-down Fermi sea will always be the minority Fermi sea in the case of nonzero polarization. The term *polarization* denotes the magnetization per particle which will be denoted by $\mathcal{P}$, thus $\mathcal{P} \equiv M/N = (N_\uparrow - N_\downarrow)/N$. The terms coverage and areal density (N/L^2) are used interchangeably. The system is assumed to be at some finite but low temperature T in the

sense that $T \ll T_{\mathrm{F}\downarrow}$. The derivation of the dispersion relations and attenuation of the collective excitations proceeds as in three dimensions, beginning with Landau's linearized kinetic equation[16]

$$\frac{\delta}{\delta t}\delta n_{\mathbf{p},\sigma}(\mathbf{r},t) + \mathbf{v}_{\mathbf{p},\sigma}\cdot\nabla_{\mathbf{r}}\delta n_{\mathbf{p},\sigma}(\mathbf{r},t) - \nabla_{\mathbf{p}} n^0_{\mathbf{p},\sigma}(\mathbf{r},t)\sum_{\mathbf{p}',\sigma'} f^{\sigma\sigma'}_{\mathbf{p}\mathbf{p}'}\nabla_{\mathbf{r}}\delta n_{\mathbf{p},\sigma}(\mathbf{r},t) = I[n_{\mathbf{p},\sigma}], \quad (2.1)$$

where $\mathbf{v}_{\mathbf{p},\sigma} \equiv \nabla_{\mathbf{p}}\epsilon_{\mathbf{p},\sigma}$ is the Fermi velocity for the σ-spin state, $f^{\sigma\sigma'}_{\mathbf{p}\mathbf{p}'} = \delta^2 E/\delta n_{\mathbf{p},\sigma}\delta n_{\mathbf{p}',\sigma'}$ are the Landau parameters, and $I[n_{\mathbf{k}',\sigma'}]$ is the collision integral. For small oscillations, we can assume traveling wave solutions for the excitations $\delta n_{\mathbf{p},\sigma}(\mathbf{r},t) = \delta n_{\mathbf{p},\sigma}(\mathbf{q},\omega)\exp[i(\mathbf{q}\cdot\mathbf{r} - \omega t)]$. The kinetic equation (2.1) reduces to

$$\left(q v_{\mathrm{F}}^{\sigma}\cos\theta - \omega\right)\nu_{\sigma}(\theta) + (q\cos\theta) \times \sum_{\mathbf{p}'\sigma'} f^{\sigma\sigma'}_{\mathbf{p}\mathbf{p}'}\,\delta\left(\epsilon_{\mathrm{F}}^{\sigma'} - \epsilon_{\mathbf{p}'\sigma'}\right)v_{\mathrm{F}}^{\sigma'}\nu_{\sigma'}(\theta') = -\frac{1}{i\tau_{\sigma}}[\nu_{\sigma}(\theta) - \langle\nu_{\sigma}(\theta)\rangle - 2\langle\nu_{\sigma}(\theta)\cos\theta\rangle\cos\theta], \quad (2.2)$$

where $\nu_{\sigma}(\theta)$ is the σth Fermi-surface distortion introduced in the usual way:

$$\delta n_{\mathbf{p},\sigma}(\mathbf{q},\omega) = -\delta\left(\epsilon_{\mathrm{F}}^{\sigma} - \epsilon_{\mathbf{p}\sigma}\right)v_{\mathrm{F}}^{\sigma}\nu_{\sigma}(\theta), \quad (2.3)$$

and θ is the angle between $\mathbf{p}$ and $\mathbf{q}$. In addition, we have written the collision integral in the relaxation-time approximation:

$$I[n_{\mathbf{p},\sigma}] = -\frac{1}{\tau_{\sigma}}[\delta n_{\mathbf{p},\sigma} - \langle\delta n_{\mathbf{p},\sigma}\rangle - 2\langle\delta n_{\mathbf{p},\sigma}\cos\theta\rangle\cos\theta]. \quad (2.4)$$

The second and third terms are added to ensure conservation of particle number, energy, and momentum.[12] The angular brackets are angular averages for two dimensions: $\langle\ldots\rangle \equiv (1/2\pi)\int_0^{2\pi}\ldots d\theta$. In Fig. 11 of LAM, we show explicitly the angular distortions of the Fermi surfaces as a function of polarization due to the presence of a zero-sound excitation.

The expression (2.2) can be simplified by introducing Fourier decompositions for the angle-dependent quantities

$$\nu_{\sigma}(\theta) = \sum_{\ell=0}^{\infty}\alpha_{\ell}\nu_{\ell}^{\sigma}\cos(\ell\theta_{\mathbf{pq}}) \equiv \sum_{\ell=0}^{\infty}\alpha_{\ell}\nu_{\ell}^{\sigma}T_{\ell}(\cos\theta_{\mathbf{pq}}), \quad (2.5a)$$

$$f^{\sigma\sigma'}_{\mathbf{p}\mathbf{p}'} = \sum_{\ell=0}^{\infty}\alpha_{\ell}f_{\ell}^{\sigma\sigma'}\cos(\ell\theta_{\mathbf{pp}'}) \equiv \sum_{\ell=0}^{\infty}\alpha_{\ell}f_{\ell}^{\sigma\sigma'}T_{\ell}[\cos(\theta_{\mathbf{pp}'})]. \quad (2.5b)$$

The constants α_{ℓ} are defined by

$$\alpha_{\ell} = \begin{cases} 1 & \text{if} \quad \ell = 0, \\ 2 & \text{if} \quad \ell \geqslant 1. \end{cases} \quad (2.6)$$

The quantities $T_{\ell}(\cos\theta) \equiv \cos(\ell\theta)$ are Chebyshev polynomials of the first kind[17] and were introduced for convenience in LAM. It was pointed out that integrals over θ from 0 to 2π can be replaced with integrals over $x \equiv \cos\theta$ from -1 to $+1$ by simply introducing the weight function $w(x) = 1/\sqrt{1-x^2}$ and multiplying by a factor of 2. This is valid whenever the function involved is real, even in θ, and periodic in θ with a period of 2π, which is the case for all functions needed in this work. There is no calculational advantage of this second representation. However, when using these variables, expressions in two dimensions become very similar to the familiar expressions in three dimensions by substituting Chebyshev polynomials for Legendre polynomials. After performing the indicated integrations, we find

$$\left(q v_{\mathrm{F}}^{\sigma}\cos\theta - \omega\right)\nu_{\sigma}(\theta) + q\cos\theta\sum_{\sigma'}v_{\mathrm{F}}^{\sigma'}N_0^{\sigma'}\sum_{\ell=0}^{\infty}\alpha_{\ell}f_{\ell}^{\sigma\sigma'}\nu_{\ell}^{\sigma'}T_{\ell}(\cos\theta) = -\frac{1}{i\tau_{\sigma}}\left[\nu_{\sigma}(\theta) - \nu_0^{\sigma} - 2\nu_1^{\sigma}\cos\theta\right], \quad (2.7)$$

where the *single* spin-state density of states is defined as

$$N_0^{\sigma} = \frac{m_{\sigma}^*}{m}\tilde{N}_0, \quad (2.8a)$$

$$\tilde{N}_0 \equiv \frac{mL^2}{2\pi\hbar^2}. \quad (2.8b)$$

The quantity $\tilde{N}_0$, the bare single spin-state density of states, will be used extensively in the following section. In Eq. (2.7), the wave vector q is a manifestly complex object with real and imaginary parts defined by

$$q = q_1 + iq_2, \quad (2.9)$$

where q_1 and q_2 are both real. In Secs. II A, II B, and II C, we will obtain analytic expressions for the dimensionless speed of sound $s = \omega/(q_1 v_{\mathrm{F}})$ and the attenuation $\mathrm{Im}(q) \equiv q_2$ in the cases of zero polarization, arbitrary polarization, and full polarization, respectively. The question of whether s is zero sound or first sound will depend on whether $\omega\tau \gg 1$ or $\omega\tau \ll 1$. Expressions for the collision frequency will be derived in Sec. III. The numerical solutions are obtained with Eq. (2.7) truncated after the $\ell = 1$ contribution. In Ref. 10, it was shown that this truncation yields accurate sound speeds.

A. Zero polarization

In this section, we shall derive the low-temperature results for sound propagation speed and attenuation in the limit of zero polarization. The general results for arbitrary polarization are presented in Sec. II B. We are proceeding in this manner for two reasons. First, zero polarization is the most important limit for the ^{3}He thin-film system. Second, the results at zero polarization can be presented as simple analytic expressions. For general polarization, we also have analytic expressions for the speed of sound and attenuation; however, they are implicit equations even in the ballistic and hydrodynamic limits and need to be solved numerically. The basic approach is the same for both zero and general polarization, thus this section can introduce the methodology within the framework of a simple but important limiting system. We wish to stress that the zero-polarization limit of the kinetic equation does not require a special derivation, and indeed we shall show that it can also be obtained from the general results. We note, however, that the situation is not so simple for the collision time as will be discussed in Sec. III.

For zero polarization, the kinetic equation (2.7) can be written as

$$\left(q v_{\mathrm{F}} \cos\theta - \omega + \frac{1}{i\tau}\right) \nu(\theta) + q v_{\mathrm{F}} \cos\theta \left[\left(F_0^s \nu_0 + 2F_1^s \nu_1 \cos\theta\right)\right] = \frac{1}{i\tau}(\nu_0 + 2\nu_1 \cos\theta). \tag{2.10}$$

The symmetric and antisymmetric Landau parameters used in the zero-polarization limit are defined as usual by

$$2N_0^\sigma f_\ell^{\sigma\sigma'} = F_\ell^s + \sigma\sigma' F_\ell^a, \tag{2.11}$$

where for this definition we associate $\sigma(\uparrow) = +1$, and $\sigma(\downarrow) = -1$. The Landau parameters that appear in Eq. (2.10) are the usual dimensionless Landau parameters scaled with the *two* spin-state density of states. Two spin-state Landau parameters are only used in the zero-polarization case.

We now rewrite Eq. (2.10) as an equation for $\nu(\theta)$ in preparation for taking moments with respect to $T_0(x) = 1$ and $T_1(x) = \cos x$:

$$\nu(\theta) = \frac{\nu_0}{\Sigma(\cos\theta - \xi)} + \left(\frac{2\nu_1}{\Sigma} - F_0^s \nu_0\right) \frac{\cos\theta}{\cos\theta - \xi} - 2F_1^s \nu_1 \frac{\cos^2\theta}{\cos\theta - \xi}. \tag{2.12}$$

Following KA, we introduce some convenient notation in Eq. (2.12):

$$\Sigma = i\tau q v_{\mathrm{F}}, \tag{2.13a}$$

$$\xi = \frac{\omega}{q v_{\mathrm{F}}} - \frac{1}{i\tau q v_{\mathrm{F}}} = \frac{\omega}{q v_{\mathrm{F}}} - \frac{1}{\Sigma}, \tag{2.13b}$$

and we especially note that $\Sigma\xi = i\omega\tau - 1$. (2.13c)

Taking $\ell = 0$ and 1 moments of Eq. (2.12) and rearranging in matrix form

$$\left(1 + F_0^s I^{(1)} - \frac{I^{(0)}}{\Sigma}\right)\nu_0 + 2\left(F_1^s I^{(2)} - \frac{I^{(1)}}{\Sigma}\right)\nu_1 = 0, \tag{2.14a}$$

$$\left(F_0^s I^{(2)} - \frac{I^{(1)}}{\Sigma}\right)\nu_0 + \left(1 + 2F_1^s I^{(3)} - \frac{2}{\Sigma} I^{(2)}\right)\nu_1 = 0, \tag{2.14b}$$

where in general the integrals that appear in (2.14) are defined by

$$I^{(n)} \equiv \frac{1}{2\pi}\int_0^{2\pi} d\theta \frac{\cos^n\theta}{\cos\theta - \xi}, \tag{2.15}$$

and where it is understood that ξ is a complex variable. The integrations can be performed analytically, and we find

$$I^{(0)} = -\frac{1 + g(\xi)}{\xi}, \tag{2.16a}$$

$$I^{(1)} = -g(\xi), \tag{2.16b}$$

$$I^{(2)} = -\xi g(\xi), \tag{2.16c}$$

$$I^{(3)} = \frac{1}{2} - \xi^2 g(\xi). \tag{2.16d}$$

We note that in Ref. 9 it was shown that when ξ is real the integral vanishes unless $|\xi| > 1$. The important function $g(\xi)$ is defined by

$$g(\xi) \equiv \frac{\xi}{\sqrt{\xi^2 - 1}} - 1. \tag{2.17}$$

If we now set the determinant of the coefficients in Eq. (2.14) equal to zero, we obtain the general result for the complex speed of sound at zero polarization:

$$\left(1 + \frac{1}{\Sigma\xi}\right)\left(1 + F_1^s\right) - \left[\left(1 + F_1^s\right)\left(F_0^s - \frac{1}{\Sigma\xi}\right) + 2\xi^2\left(1 + \frac{1}{\Sigma\xi}\right)\left(F_1^s - \frac{1}{\Sigma\xi}\right)\right] g(\xi) = 0. \tag{2.18}$$

1. Zero sound

Zero sound propagates in the ballistic regime $\omega\tau \gg 1$. Thus, from Eq. (2.13c), we look for solutions of (2.18) in the limit $|\Sigma\xi| \approx |\omega\tau| \gg 1$. We now need to expand the complex sound speed ξ into its real and imaginary parts. From Eq. (2.13b), we have

$$\xi = \frac{\omega}{q v_{\mathrm{F}}} + \frac{i}{\tau q v_{\mathrm{F}}} \equiv s(1 + i\xi'), \tag{2.19}$$

where s, the dimensionless zero-sound speed of propagation, and ξ' are both real. The wave vector $q = q_1 + iq_2$ is also complex, and so we find

$$\xi = s\left[1 + i\left(\frac{1}{\omega\tau} - \frac{q_2}{q_1}\right)\right]. \tag{2.20}$$

By inspection, we can identify the propagation speed $s = \omega/(q_1 v_{\mathrm{F}})$ and the attenuation $q_2/q_1 = 1/(\omega\tau) - \xi'$. We assume that $q_2/q_1 \ll 1$ and thus in this regime we must have $\xi' \ll 1$. Expanding Eq. (2.17) to lowest order in ξ' yields

$$g(\xi) = g(s) - \left(\frac{g(s) + 1}{s^2 - 1}\right) i\xi'. \tag{2.21}$$

Then, from Eq. (2.18), we find for the propagation speed and the attenuation, respectively,

$$g(s) = \frac{1 + F_1^s}{\left(1 + F_1^s\right)F_0^s + 2s^2 F_1^s}, \tag{2.22}$$

$$\frac{q_2}{q_1} = \frac{1}{\omega\tau}\left[1 - \frac{\left(1 + F_1^s\right)[1 + g(s)] + 2s^2\left(1 - F_1^s\right)g(s)}{\frac{\left(1 + F_1^s\right)}{g(s)}\frac{[1 + g(s)]}{s^2 - 1} - 4s^2 F_1^s g(s)}\right]. \tag{2.23}$$

In the simplest approximation, $F_1^s = 0$ and $g(s) = 1/F_0^s$ in agreement with previous results.[10]

2. First sound

In the hydrodynamic regime, $\omega\tau \ll 1$. Thus, $\frac{1}{\Sigma\xi} \approx -1 - i\omega\tau$, and $|\xi| \gg 1$. Thus, in this regime, we can expand quantities in powers of $1/\xi$. From Eq. (2.17),

$$g(\xi) \approx \frac{1}{2\xi^2} + \frac{3}{8}\frac{1}{\xi^4}. \tag{2.24}$$

If we substitute this back into Eq. (2.18), we find

$$\left(1+\frac{1}{\Sigma\xi}\right)^2=\frac{1}{2\xi^2}\left[\left(1+F_1^s\right)\left(F_0^s-\frac{1}{\Sigma\xi}\right)+\frac{3}{2}\left(1+\frac{1}{\Sigma\xi}\right)\left(F_1^s-\frac{1}{\Sigma\xi}\right)\right]. \quad (2.25)$$

In order to obtain quantities of $O(1)$, we multiply both sides of (2.25) by ξ^2:

$$\left(\frac{\omega}{q v_{\mathrm{F}}}\right)^2=\frac{1}{2}\left[\left(1+F_1^s\right)\left(1+F_0^s-i\frac{\omega\tau}{2}\right)\right]. \quad (2.26)$$

Then, separating into real and imaginary components by using $q=q_1+iq_2$, we obtain the propagation speed and the attenuation:

$$s^2=\frac{1}{2}\left(1+F_0^s\right)\left(1+F_1^s\right), \quad (2.27)$$

$$q_2/q_1=\frac{\omega\tau}{4\left(1+F_0^s\right)}. \quad (2.28)$$

B. Arbitrary polarization

The calculation for arbitrary polarization proceeds in the same manner as that for zero polarization with the considerable additional complexity of having to solve a 4×4 determinant instead of the 2×2. The state-dependent generalization of Eq. (2.12) is given by

$$\nu_\sigma(\theta)=-\frac{\nu_0^\sigma}{\Sigma_\sigma(\xi_\sigma-\cos\theta)}+\left(\frac{m_\sigma^*}{m}\tilde{F}_0^{\sigma\sigma}\nu_0^\sigma+\frac{v_{\mathrm{F}}^{-\sigma}}{v_{\mathrm{F}}^\sigma}\frac{m_{-\sigma}^*}{m}\tilde{F}_0^{\sigma-\sigma}\nu_0^{-\sigma}-\frac{2\nu_1^\sigma}{\Sigma^\sigma}\right)\frac{\cos\theta}{\xi_\sigma-\cos\theta}+2\left(\frac{m_\sigma^*}{m}\tilde{F}_1^{\sigma\sigma}\nu_1^\sigma+\frac{v_{\mathrm{F}}^{-\sigma}}{v_{\mathrm{F}}^\sigma}\frac{m_{-\sigma}^*}{m}\tilde{F}_1^{\sigma-\sigma}\nu_1^{-\sigma}\right)\frac{\cos^2\theta}{\xi_\sigma-\cos\theta}. \quad (2.29)$$

The tilde notation for the dimensionless Landau parameters indicates that these parameters are scaled with the bare single spin-state density of states as introduced in LAM: $\tilde{F}_\ell^{\sigma\sigma'}=\tilde{N}_0 f_\ell^{\sigma\sigma'}$. The state-dependent versions of the parameters introduced in Eqs. (2.13) are given by

$$\Sigma_\sigma\equiv i\tau_\sigma q v_{\mathrm{F}}^\sigma, \quad (2.30a)$$

$$\xi_\sigma\equiv\frac{\omega}{q v_{\mathrm{F}}^\sigma}-\frac{1}{i\tau_\sigma q v_{\mathrm{F}}^\sigma}, \quad (2.30b)$$

$$g_\sigma\equiv g(\xi_\sigma). \quad (2.30c)$$

Using Eqs. (2.16), we take $\ell=0$ and 1 moments of Eq. (2.29) to find the generalizations of Eqs. (2.14):

$$\left(-1-\frac{1+g_\sigma}{\xi_\sigma\Sigma_\sigma}+\frac{m_\sigma^*}{m}\tilde{F}_0^{\sigma\sigma}g_\sigma\right)\nu_0^\sigma+\left(\frac{v_{\mathrm{F}}^{-\sigma}}{v_{\mathrm{F}}^\sigma}\frac{m_{-\sigma}^*}{m}\tilde{F}_0^{\sigma-\sigma}g_\sigma\right)\nu_0^{-\sigma}+2\left(\frac{m_\sigma^*}{m}\tilde{F}_1^{\sigma\sigma}\xi_\sigma g_\sigma-\frac{g_\sigma}{\Sigma_\sigma}\right)\nu_1^\sigma+2\left(\frac{v_{\mathrm{F}}^{-\sigma}}{v_{\mathrm{F}}^\sigma}\frac{m_{-\sigma}^*}{m}\tilde{F}_1^{\sigma-\sigma}\xi_\sigma g_\sigma\right)\nu_1^{-\sigma}=0, \quad (2.31a)$$

$$\left(-\frac{g_\sigma}{\Sigma_\sigma}+\frac{m_\sigma^*}{m}\tilde{F}_0^{\sigma\sigma}\xi_\sigma g_\sigma\right)\nu_0^\sigma+\left(\frac{v_{\mathrm{F}}^{-\sigma}}{v_{\mathrm{F}}^\sigma}\frac{m_{-\sigma}^*}{m}\tilde{F}_0^{\sigma-\sigma}\xi_\sigma g_\sigma\right)\nu_0^{-\sigma}+2\left[\frac{m_\sigma^*}{m}\tilde{F}_1^{\sigma\sigma}\left(\xi_\sigma^2 g_\sigma-\frac{1}{2}\right)-\frac{\xi_\sigma g_\sigma}{\Sigma_\sigma}-\frac{1}{2}\right]\nu_1^\sigma+2\left[\frac{v_{\mathrm{F}}^{-\sigma}}{v_{\mathrm{F}}^\sigma}\frac{m_{-\sigma}^*}{m}\tilde{F}_1^{\sigma-\sigma}\left(\xi_\sigma^2 g_\sigma-\frac{1}{2}\right)\right]\nu_1^{-\sigma}=0. \quad (2.31b)$$

Setting the determinant of the coefficients equal to zero, we find after some algebra

$$\begin{aligned}&\left\{\left(1+\frac{1}{\Sigma_\uparrow\xi_\uparrow}\right)\left[\left(1+\frac{2\xi_\uparrow g_\uparrow}{\Sigma_\uparrow}\right)+(1-2\xi_\uparrow^2 g_\uparrow)F_1^{\uparrow\uparrow}\right]+\left(\frac{1}{\Sigma_\uparrow\xi_\uparrow}-F_0^{\uparrow\uparrow}\right)(1+F_1^{\uparrow\uparrow})g_\uparrow\right\}\\&\times\left\{\left(1+\frac{1}{\Sigma_\downarrow\xi_\downarrow}\right)\left[\left(1+\frac{2\xi_\downarrow g_\downarrow}{\Sigma_\downarrow}\right)+(1-2\xi_\downarrow^2 g_\downarrow)F_1^{\downarrow\downarrow}\right]+\left(\frac{1}{\Sigma_\downarrow\xi_\downarrow}-F_0^{\downarrow\downarrow}\right)(1+F_1^{\downarrow\downarrow})g_\downarrow\right\}\\&-(F_0^{\uparrow\downarrow})^2 g_\uparrow g_\downarrow[(1+F_1^{\uparrow\uparrow})(1+F_1^{\downarrow\downarrow})-(F_1^{\uparrow\downarrow})^2]-4F_0^{\uparrow\downarrow}F_1^{\uparrow\downarrow}\left(1+\frac{1}{\Sigma_\uparrow\xi_\uparrow}\right)\left(1+\frac{1}{\Sigma_\downarrow\xi_\downarrow}\right)\xi_\uparrow g_\uparrow\xi_\downarrow g_\downarrow\\&-(F_1^{\uparrow\downarrow})^2\left[\left(1+\frac{1}{\Sigma_\uparrow\xi_\uparrow}\right)(1-2\xi_\uparrow^2 g_\uparrow)+\left(\frac{1}{\Sigma_\uparrow\xi_\uparrow}-F_0^{\uparrow\uparrow}\right)g_\uparrow\right]\\&\times\left[\left(1+\frac{1}{\Sigma_\downarrow\xi_\downarrow}\right)(1-2\xi_\downarrow^2 g_\downarrow)+\left(\frac{1}{\Sigma_\downarrow\xi_\downarrow}-F_0^{\downarrow\downarrow}\right)g_\downarrow\right]=0.\end{aligned} \quad (2.32)$$

For convenience, we introduced a hybrid notation in Eq. (2.32) to absorb some of the effective mass factors:

$$F_\ell^{\sigma\sigma}\equiv\frac{m_\sigma^*}{m}\tilde{F}_\ell^{\sigma\sigma}, \quad \left(F_\ell^{\sigma-\sigma}\right)^2\equiv\frac{m_\uparrow^* m_\downarrow^*}{m^2}\left(\tilde{F}_\ell^{\sigma-\sigma}\right)^2. \quad (2.33)$$

It is convenient at this point to examine Eq. (2.32) in the limit of zero polarization. We then find

$$\left\{\left(1+\frac{1}{\Sigma_\uparrow\xi_\uparrow}\right)\left[\left(1+\frac{2\xi_\uparrow g_\uparrow}{\Sigma_\uparrow}\right)+(1-2\xi_\uparrow^2 g_\uparrow)F_1^s\right]+\left(\frac{1}{\Sigma_\uparrow\xi_\uparrow}-F_0^s\right)(1+F_1^s)g_\uparrow\right\}$$
$$\times\left\{\left(1+\frac{1}{\Sigma_\downarrow\xi_\downarrow}\right)\left[\left(1+\frac{2\xi_\downarrow g_\downarrow}{\Sigma_\downarrow}\right)+(1-2\xi_\downarrow^2 g_\downarrow)F_1^a\right]+\left(\frac{1}{\Sigma_\downarrow\xi_\downarrow}-F_0^a\right)(1+F_1^a)g_\downarrow\right\}=0, \tag{2.34}$$

where at zero polarization the arrow subscripts are not needed but have been retained to make comparison with (2.32) easier. In the ballistic limit, the first term in curly brackets corresponds to zero sound, and the second term in curly brackets corresponds to spin zero sound. The symmetric and antisymmetric Landau parameters are the two spin-state scaled parameters as defined in Eq. (2.11). Each of the terms in curly brackets is in agreement with the previously derived zero-polarization limit Eq. (2.18). In the same manner, the full-polarization limit that will be discussed in the following follows directly from Eq. (2.31a).

1. Zero sound

In the ballistic regime, $\omega\tau_\sigma \gg 1$, and so we expand (2.32) in powers of $\frac{1}{\omega\tau_\sigma}$. We will need the following asymptotic results:

$$\frac{1}{\Sigma_\uparrow\xi_\uparrow}\sim\frac{1}{i\omega\tau_\uparrow}, \tag{2.35a}$$
$$\xi_\uparrow\sim s_\uparrow(1+i\xi'_\uparrow), \tag{2.35b}$$
$$g(\xi_\uparrow)\sim g(s_\uparrow)+is_\uparrow g^{(1)}(s_\uparrow)\xi'_\uparrow, \tag{2.35c}$$
$$\left(1+\frac{1}{\Sigma_\uparrow\xi_\uparrow}\right)\left(1+\frac{2\xi_\uparrow g_\uparrow}{\Sigma_\uparrow}\right)\sim 1-\left[1+2s_\uparrow^2 g(s_\uparrow)\right]\frac{i}{\omega\tau_\uparrow}, \tag{2.35d}$$
$$\left(1+\frac{1}{\Sigma_\uparrow\xi_\uparrow}\right)(1-2\xi_\uparrow^2 g_\uparrow)$$
$$\sim[1-2s_\uparrow^2 g(s_\uparrow)]-\frac{i}{\omega\tau_\uparrow}[1+2s_\uparrow^2[g(s_\uparrow)+h_\uparrow]]$$
$$+2is_\uparrow^2[2g(s_\uparrow)+h_\uparrow]\frac{q_2}{q_1}, \tag{2.35e}$$
$$\left(\frac{1}{\Sigma_\uparrow\xi_\uparrow}-F_0^{\uparrow\uparrow}\right)g_\uparrow$$
$$\sim -F_0^{\uparrow\uparrow}g(s_\uparrow)-i\left[[F_0^{\uparrow\uparrow}h_\uparrow+g(s_\uparrow)]\frac{1}{\omega\tau_\uparrow}-F_0^{\uparrow\uparrow}h_\uparrow\frac{q_2}{q_1}\right]. \tag{2.35f}$$

The following definitions were introduced in Eqs. (2.35):

$$s_\uparrow\equiv\frac{\omega}{q_1 v_{\mathrm{F}\uparrow}}, \tag{2.36a}$$
$$h_\uparrow\equiv s_\uparrow g^{(1)}(s_\uparrow), \tag{2.36b}$$
$$g_\uparrow^{(1)}\equiv\left(\frac{\partial g_\uparrow}{\partial s_\uparrow}\right)_{\xi'=0}, \tag{2.36c}$$
$$\xi'_\uparrow\equiv\frac{1}{\omega\tau_\uparrow}-\frac{q_2}{q_1}. \tag{2.36d}$$

Equivalent definitions hold for down-spin entities.

Expanding (2.32) yields the relation that determines s_σ, the zero-sound speeds:

$$[1-F_0^{\uparrow\uparrow}g(s_\uparrow)+F_1^{\uparrow\uparrow}A_\uparrow][1-F_0^{\downarrow\downarrow}g(s_\downarrow)+F_1^{\downarrow\downarrow}A_\downarrow]$$
$$-(F_0^{\uparrow\downarrow})^2[(1+F_1^{\uparrow\uparrow})(1+F_1^{\downarrow\downarrow})-(F_1^{\uparrow\downarrow})^2]g(s_\uparrow)g(s_\downarrow)$$
$$-(F_1^{\uparrow\downarrow})^2A_\uparrow A_\downarrow-4F_0^{\uparrow\downarrow}F_1^{\uparrow\downarrow}s_\uparrow s_\downarrow g(s_\uparrow)g(s_\downarrow)=0, \tag{2.37}$$

and we have defined

$$A_\sigma\equiv 1-2s_\sigma^2 g(s_\sigma)-F_0^{\sigma\sigma}g(s_\sigma).$$

Similarly, the attenuation can be written as

$$q_2/q_1=\frac{N_\uparrow/(\omega\tau_\uparrow)+N_\downarrow/(\omega\tau_\downarrow)}{D}, \tag{2.38}$$

where

$$N_\uparrow=[1-F_0^{\downarrow\downarrow}g(s_\downarrow)+A_\downarrow F_1^{\downarrow\downarrow}]\left(c^0_{\tau,\uparrow}+c^1_{\tau,\uparrow}F_1^{\uparrow\uparrow}\right)$$
$$+(F_0^{\uparrow\downarrow})^2[(1+F_1^{\uparrow\uparrow})(1+F_1^{\downarrow\downarrow})-(F_1^{\uparrow\downarrow})^2]h_\uparrow g(s_\downarrow)$$
$$-(F_1^{\uparrow\downarrow})^2A_\downarrow c^1_{\tau,\uparrow}+4F_0^{\uparrow\downarrow}F_1^{\uparrow\downarrow}s_\uparrow s_\downarrow g(s_\downarrow)h_\uparrow, \tag{2.39}$$

$$D=[1-F_0^{\uparrow\uparrow}g(s_\uparrow)+A_\uparrow F_1^{\uparrow\uparrow}]\left(F_0^{\downarrow\downarrow}h_\downarrow+c^1_{q,\downarrow}F_1^{\downarrow\downarrow}\right)$$
$$+[1-F_0^{\downarrow\downarrow}g(s_\downarrow)+A_\downarrow F_1^{\downarrow\downarrow}]\left(F_0^{\uparrow\uparrow}h_\uparrow+c^1_{q,\uparrow}F_1^{\uparrow\uparrow}\right)$$
$$+(F_0^{\uparrow\downarrow})^2[(1+F_1^{\uparrow\uparrow})(1+F_1^{\downarrow\downarrow})-(F_1^{\uparrow\downarrow})^2]$$
$$\times[h_\uparrow g(s_\downarrow)+h_\downarrow g(s_\uparrow)]$$
$$-(F_1^{\uparrow\downarrow})^2\left(A_\uparrow c^1_{q,\downarrow}+A_\downarrow c^1_{q,\uparrow}\right)+4F_0^{\uparrow\downarrow}F_1^{\uparrow\downarrow}s_\uparrow s_\downarrow$$
$$\times[g(s_\downarrow)h_\uparrow+g(s_\uparrow)h_\downarrow+2g(s_\uparrow)g(s_\downarrow)], \tag{2.40}$$

and for $N_\downarrow$ simply reverse all the spins in (2.39). For convenience, we have defined the following quantities:

$$c^0_{\tau,\sigma}\equiv 1+\left(2s_\sigma^2+1\right)g(s_\sigma)+F_0^{\sigma\sigma}h_\sigma, \tag{2.41a}$$
$$c^1_{\tau,\sigma}\equiv 1+2s_\sigma^2[g(s_\sigma)+h_\sigma]+g(s_\sigma)+F_0^{\sigma\sigma}h_\sigma, \tag{2.41b}$$
$$c^1_{q,\sigma}\equiv 2s_\sigma^2[2g(s_\sigma)+h_\sigma]+F_0^{\sigma\sigma}h_\sigma. \tag{2.41c}$$

2. First sound

As at zero polarization in Sec. II A, for first sound we need to find solutions of the linearized kinetic equation in the hydrodynamic limit $\omega\tau_\sigma \ll 1$. The fundamental determinant

Eq. (2.32) can be rewritten as

$$\left\{\left(1+\frac{1}{\Sigma_\uparrow\xi_\uparrow}\right)\left[\left(1+\frac{1}{\Sigma_\uparrow\xi_\uparrow}\right)+(2\xi_\uparrow^2 g_\uparrow-1)\left(\frac{1}{\Sigma_\uparrow\xi_\uparrow}-F_1^{\uparrow\uparrow}\right)\right]+(1+F_1^{\uparrow\uparrow})\left(\frac{1}{\Sigma_\uparrow\xi_\uparrow}-F_0^{\uparrow\uparrow}\right)g_\uparrow\right\}$$
$$\times\left\{\left(1+\frac{1}{\Sigma_\downarrow\xi_\downarrow}\right)\left[\left(1+\frac{1}{\Sigma_\downarrow\xi_\downarrow}\right)+(2\xi_\downarrow^2 g_\downarrow-1)\left(\frac{1}{\Sigma_\downarrow\xi_\downarrow}-F_1^{\downarrow\downarrow}\right)\right]+(1+F_1^{\downarrow\downarrow})\left(\frac{1}{\Sigma_\downarrow\xi_\downarrow}-F_0^{\downarrow\downarrow}\right)g_\downarrow\right\}$$
$$-(F_0^{\uparrow\downarrow})^2 g_\uparrow g_\downarrow[(1+F_1^{\uparrow\uparrow})(1+F_1^{\downarrow\downarrow})-(F_1^{\uparrow\downarrow})^2]-4F_0^{\uparrow\downarrow}F_1^{\uparrow\downarrow}\left[\xi_\uparrow\left(1+\frac{1}{\Sigma_\uparrow\xi_\uparrow}\right)\xi_\downarrow\left(1+\frac{1}{\Sigma_\downarrow\xi_\downarrow}\right)\right]g_\uparrow g_\downarrow$$
$$-(F_1^{\uparrow\downarrow})^2\left[\left(1+\frac{1}{\Sigma_\uparrow\xi_\uparrow}\right)(1-2\xi_\uparrow^2 g_\uparrow)+\left(\frac{1}{\Sigma_\uparrow\xi_\uparrow}-F_0^{\uparrow\uparrow}\right)g_\uparrow\right]$$
$$\times\left[\left(1+\frac{1}{\Sigma_\downarrow\xi_\downarrow}\right)(1-2\xi_\downarrow^2 g_\downarrow)+\left(\frac{1}{\Sigma_\downarrow\xi_\downarrow}-F_0^{\downarrow\downarrow}\right)g_\downarrow\right]=0. \tag{2.42}$$

We will need the following asymptotic results:

$$g_\uparrow\sim\frac{1}{2\xi_\uparrow^2}\left(1+\frac{3}{4}\frac{1}{\xi_\uparrow^2}\right), \tag{2.43a}$$
$$\frac{1}{\Sigma_\uparrow\xi_\uparrow}\sim-(1+i\omega\tau_\uparrow). \tag{2.43b}$$

The first sound speed $s_1^\sigma\equiv c_1^\sigma/v_F^\sigma\equiv\omega/(q_1 v_F^\sigma)$ is the solution of

$$[2(s_1^\uparrow)^2-(1+F_0^{\uparrow\uparrow})(1+F_1^{\uparrow\uparrow})]$$
$$\times[2(s_1^\downarrow)^2-(1+F_0^{\downarrow\downarrow})(1+F_1^{\downarrow\downarrow})]$$
$$-(F_0^{\uparrow\downarrow})^2[(1+F_1^{\uparrow\uparrow})(1+F_1^{\downarrow\downarrow})-(F_1^{\uparrow\downarrow})^2]$$
$$-(F_1^{\uparrow\downarrow})^2(1+F_0^{\uparrow\uparrow})(1+F_0^{\downarrow\downarrow})$$
$$-4F_0^{\uparrow\downarrow}F_1^{\uparrow\downarrow}s_1^\uparrow s_1^\downarrow=0. \tag{2.44}$$

The attenuation q_2/q_1 is given by

$$q_2/q_1=\frac{1}{8}\frac{N_\uparrow(\omega\tau_\uparrow)+N_\downarrow(\omega\tau_\downarrow)}{D}, \tag{2.45}$$

where the numerator and denominator in Eq. (2.45) are given by

$$N_\uparrow=2(1+F_1^{\uparrow\uparrow})(s_1^\downarrow)^2-(1+F_0^{\downarrow\downarrow})$$
$$\times[(1+F_1^{\uparrow\uparrow})(1+F_1^{\downarrow\downarrow})-(F_1^{\uparrow\downarrow})^2], \tag{2.46a}$$
$$N_\downarrow=2(1+F_1^{\downarrow\downarrow})(s_1^\uparrow)^2-(1+F_0^{\uparrow\uparrow})$$
$$\times[(1+F_1^{\downarrow\downarrow})(1+F_1^{\uparrow\uparrow})-(F_1^{\uparrow\downarrow})^2], \tag{2.46b}$$
$$D=(s_1^\uparrow)^2[2(s_1^\downarrow)^2-(1+F_0^{\downarrow\downarrow})(1+F_1^{\downarrow\downarrow})]+(s_1^\downarrow)^2[2(s_1^\uparrow)^2$$
$$-(1+F_0^{\uparrow\uparrow})(1+F_1^{\uparrow\uparrow})]-2F_0^{\uparrow\downarrow}F_1^{\uparrow\downarrow}s_1^\uparrow s_1^\downarrow. \tag{2.46c}$$

C. Full polarization

In this section, we examine sound speeds in the limit that *all* of the particles are in the spin-up Fermi sea. We note that one must be careful in trying to apply the results from Sec. II B to the *almost* complete polarized limit. Our analysis using Landau's kinetic equation is valid when $T<T_{F\sigma}$, a case that may be problematic for the minority Fermi sea.

Using the one-spin form of Eqs. (2.14), we obtain

$$\left[-\left(1+\frac{1}{\Sigma_\uparrow\xi_\uparrow}\right)+g_\uparrow\left(F_0^{\uparrow\uparrow}-\frac{1}{\Sigma_\uparrow\xi_\uparrow}\right)\right]\nu_0^\uparrow$$
$$+2\xi_\uparrow g_\uparrow\left(F_1^{\uparrow\uparrow}-\frac{1}{\Sigma_\uparrow\xi_\uparrow}\right)\nu_1^\uparrow=0, \tag{2.47}$$
$$\xi_\uparrow g_\uparrow\left(F_0^{\uparrow\uparrow}-\frac{1}{\Sigma_\uparrow\xi_\uparrow}\right)\nu_0^\uparrow$$
$$+\left[2\xi_\uparrow^2 g_\uparrow\left(F_1^{\uparrow\uparrow}-\frac{1}{\Sigma_\uparrow\xi_\uparrow}\right)-(1+F_1^{\uparrow\uparrow})\right]\nu_1^\uparrow=0. \tag{2.48}$$

We note that this also follows directly from Eq. (2.32) by setting $g_\downarrow=F_1^{\uparrow\downarrow}=0$. There are solutions when the secular determinant vanishes:

$$\left(1+\frac{1}{\Sigma_\uparrow\xi_\uparrow}\right)\left[\left(1+\frac{1}{\Sigma_\uparrow\xi_\uparrow}\right)+(2\xi_\uparrow^2 g_\uparrow-1)\left(\frac{1}{\Sigma_\uparrow\xi_\uparrow}-F_1^{\uparrow\uparrow}\right)\right]$$
$$-(1+F_1^{\uparrow\uparrow})\left(F_0^{\uparrow\uparrow}-\frac{1}{\Sigma_\uparrow\xi_\uparrow}\right)g_\uparrow=0. \tag{2.49}$$

1. Zero sound

In the ballistic regime $\omega\tau_\uparrow\gg1$, and as above the secular determinant becomes

$$[(1-F_0^{\uparrow\uparrow}g(s_\uparrow))+F_1^{\uparrow\uparrow}(1-2s_\uparrow^2 g(s_\uparrow)-F_0^{\uparrow\uparrow}g(s_\uparrow))]$$
$$-\frac{i}{\omega\tau_\uparrow}(c_{\tau\uparrow}^0+F_1^{\uparrow\uparrow}c_{\tau\uparrow}^1)+i\frac{q_2}{q_1}(F_0^{\uparrow\uparrow}h_\uparrow+F_1^{\uparrow\uparrow}c_{q\uparrow}^1)=0. \tag{2.50}$$

The dimensionless zero-sound speed $s_\uparrow$ is the solution of

$$g(s_\uparrow)=\frac{1+F_1^{\uparrow\uparrow}}{F_0^{\uparrow\uparrow}(1+F_1^{\uparrow\uparrow})+2s_\uparrow^2F_1^{\uparrow\uparrow}}. \tag{2.51}$$

In the simplest approximation $F_1^{\uparrow\uparrow}=0$, and we find

$$s_\uparrow^2=\frac{(1+F_0^{\uparrow\uparrow})^2}{1+2F_0^{\uparrow\uparrow}}, \tag{2.52}$$

in agreement with previous results.[10] The attenuation is

$$q_2/q_1 = \left[\frac{c^0_{\tau\uparrow} + F_1^{\uparrow\uparrow} c^1_{\tau\uparrow}}{F_0^{\uparrow\uparrow} h_\uparrow + F_1^{\uparrow\uparrow} c^1_{q\uparrow}}\right] \frac{1}{\omega\tau_\uparrow}. \tag{2.53}$$

2. First sound

In the hydrodynamic regime, $\omega\tau_\uparrow \ll 1$, and equivalently $\xi_\uparrow \gg 1$. Equation (2.49) can be written as

$$\left(1 + \frac{1}{\Sigma_\uparrow \xi_\uparrow}\right)^2 + (-i\omega\tau_\uparrow)\frac{3}{4}\frac{1}{\xi_\uparrow^2}[-(1 + F_1^{\uparrow\uparrow})] - (1 + F_1^{\uparrow\uparrow})\frac{1}{2\xi_\uparrow^2}[(1 + F_0^{\uparrow\uparrow}) + i\omega\tau_\uparrow] = 0. \tag{2.54}$$

This immediately yields

$$\left(\frac{\omega}{q v_F^\uparrow}\right)^2 - \frac{1}{2}(1 + F_0^{\uparrow\uparrow})(1 + F_1^{\uparrow\uparrow}) + i\omega\tau_\uparrow \frac{1 + F_1^{\uparrow\uparrow}}{4} = 0. \tag{2.55}$$

Thus, the dimensionless first sound speed is

$$s_\uparrow^2 = \tfrac{1}{2}(1 + F_0^{\uparrow\uparrow})(1 + F_1^{\uparrow\uparrow}), \tag{2.56}$$

and the attenuation is

$$q_2/q_1 = \frac{\omega\tau_\uparrow}{4(1 + F_0^{\uparrow\uparrow})}. \tag{2.57}$$

III. COLLISION TIME

In Sec. II, we derived expressions for the propagation speed and attenuation of zero sound and first sound. The results depend only on the Landau parameters and so they can be evaluated using results reported in LAM (Refs. 9–11). In order to calculate the attenuation, however, we still need to derive expressions for the collision frequency $1/\tau$. In the following two sections, we shall consider two mechanisms for quasiparticle scattering. The first, quasiparticle-quasiparticle scattering, is the same as in three dimensions. The second is quasiparticle-phonon scattering, which needs to be considered in the case of adsorbed films. We shall show that the mismatch between sound speeds and Fermi velocities even at the largest densities and polarization renders this possibility moot.

A. Quasiparticle-quasiparticle collisions

The collision frequency for the σth Fermi sea is given by[16]

$$\frac{1}{\tau_\sigma(\mathbf{p})} = \sum_{\mathbf{k},\mathbf{q}} \left[\frac{1}{2} W_{\sigma\sigma}(q) n_{\mathbf{k},\sigma} \bar{n}_{\mathbf{p}-\mathbf{q},\sigma} \bar{n}_{\mathbf{k}+\mathbf{q},\sigma} + W_{\sigma-\sigma}(q) n_{\mathbf{k},-\sigma} \bar{n}_{\mathbf{p}-\mathbf{q},\sigma} \bar{n}_{\mathbf{k}+\mathbf{q},-\sigma}\right] \times \delta(\epsilon_{\mathbf{p}} + \epsilon_{\mathbf{k}} - \epsilon_{\mathbf{k}+\mathbf{q}} - \epsilon_{\mathbf{p}-\mathbf{q}}), \tag{3.1}$$

where $n_{\mathbf{p}\sigma} \equiv 1/\{\exp[\beta(\epsilon_{\mathbf{p}\sigma} - \mu_\sigma)] + 1\}$ is the Fermi distribution function, $\beta \equiv 1/k_B T$, and μ_σ is the chemical potential for the σth Fermi sea. We have defined

$$\bar{n}_{\mathbf{p}\sigma} \equiv 1 - n_{\mathbf{p}\sigma} = \frac{1}{1 + e^{-\beta(\epsilon_{\mathbf{p}\sigma} - \mu_\sigma)}}. \tag{3.2}$$

The W terms are transition probabilities, and the factor of one-half before $W_{\sigma\sigma}$ prevents double counting. The standard treatment in three dimensions follows Abrikosov and Khalatnikov,[12] and introduces new integration variables in terms of energies and angles. These integrations are independent of one another, and in lowest order in temperature one can find a closed form expression for $1/\tau$ in terms of an angular average of the transition probability.

The change of variables introduces a factor of $1/\sin\theta$ into the integrand, and in two dimensions the subsequent integration over θ yields logarithmic singularities at 0 and π. In three dimensions, there is a canceling factor of $\sin\theta$ that appears in the Jacobian of the angular integration. This situation is discussed in detail by Miyake and Mullin[18] who offer a clever geometric solution around the problem. In this section, we shall take a different tack and proceed along the lines pioneered in the two-dimensional electron community. In particular, we shall use the approach of Giuliani and Quinn[19] that takes advantage of the similarity between the structure of Eq. (3.1) and the dynamic structure factor for an ideal Fermi gas:

$$S^0_{\sigma\sigma}(\mathbf{q},\omega) = \sum_{\mathbf{k}} n_{\mathbf{k},\sigma} \bar{n}_{\mathbf{k}+\mathbf{q},\sigma} \delta(\omega + \epsilon_{\mathbf{k},\sigma} - \epsilon_{\mathbf{k}+\mathbf{q},\sigma}), \tag{3.3}$$

where by inspection we can identify

$$\omega = \epsilon_{\mathbf{p}} - \epsilon_{\mathbf{p}-\mathbf{q}}. \tag{3.4}$$

The fluctuation-dissipation theorem allows us to rewrite the dynamic structure factor in terms of the imaginary part of the susceptibility $\chi''_\sigma(\mathbf{q},\omega)$:

$$\pi S_{\sigma\sigma}(\mathbf{q},\omega) = -\frac{\chi''_\sigma(\mathbf{q},\omega)}{1 - e^{-\beta\omega}}, \tag{3.5}$$

where we omit 0 superscripts since all the distribution functions here are for a free Fermi gas.

$\chi''_\sigma(\mathbf{q},\omega)$ for an ideal two-dimensional Fermi gas was evaluated by Stern.[20] Using

$$\chi''_\sigma(\mathbf{q},\omega) = -\pi \sum_{\mathbf{k}} (n_{\mathbf{k},\sigma} - n_{\mathbf{k}+\mathbf{q},\sigma}) \delta(\omega - \omega_{kq}), \tag{3.6}$$

where

$$\omega_{kq} \equiv \frac{kq\cos\theta_{\mathbf{kq}}}{m^*_\sigma} + \frac{q^2}{2m^*_\sigma}. \tag{3.7}$$

The integrations in (3.6) are straightforward and we find

$$\chi''_\sigma(\mathbf{q},\omega) = -\left(\frac{2m^*_\sigma \pi}{h^2 q}\right)\left[\sqrt{k_{F\sigma}^2 - \left(\frac{m^*_\sigma\omega}{q} - \frac{q}{2}\right)^2} \times \theta\left(k_{F\sigma} - \left|\frac{m^*_\sigma\omega}{q} - \frac{q}{2}\right|\right) - \sqrt{k_{F\sigma}^2 - \left(\frac{m^*_\sigma\omega}{q} + \frac{q}{2}\right)^2}\,\theta\left(k_{F\sigma} - \left|\frac{m^*_\sigma\omega}{q} + \frac{q}{2}\right|\right)\right], \tag{3.8}$$

where $\theta(\ldots)$ are Heaviside step functions. Equation (3.8) is the $T = 0$ K limit which should serve our purposes.

For convenience, we divide the calculation into two parts:

$$\frac{1}{\tau_\sigma} = \frac{1}{\tau_{\sigma\sigma}} + \frac{1}{\tau_{\sigma-\sigma}}, \tag{3.9}$$

where

$$\frac{1}{\tau_{\sigma\sigma}} \equiv -\left(\frac{1}{\pi}\right)\sum_{\mathbf{q}}\frac{1}{2}W_{\sigma\sigma}(q)\overline{n}_{\mathbf{p}-\mathbf{q},\sigma}\frac{\chi''_\sigma(\mathbf{q},\omega)}{(1-e^{-\beta\omega})}, \tag{3.10a}$$

$$\frac{1}{\tau_{\sigma-\sigma}} \equiv -\left(\frac{1}{\pi}\right)\sum_{\mathbf{q}}W_{\sigma-\sigma}(q)\overline{n}_{\mathbf{p}-\mathbf{q},\sigma}\frac{\chi''_{-\sigma}(\mathbf{q},\omega)}{(1-e^{-\beta\omega})}. \tag{3.10b}$$

We begin by analyzing $(1/\tau_{\sigma-\sigma})$. Using the definition of ω [Eq. (3.4)], Eq. (3.10b) can be rewritten as

$$\frac{1}{\tau_{\sigma-\sigma}} = -\frac{1}{\pi h^2}\int_0^\infty dq\, q W_{\sigma-\sigma}(q)\int_{-\infty}^\infty d\omega\frac{\chi''_{-\sigma}(\mathbf{q},\omega)}{(1-e^{-\beta\omega})(1+e^{-\beta(\epsilon_{\mathbf{p},\sigma}-\mu_\sigma-\omega)})}\int_0^{2\pi}d\theta_{\mathbf{pq}}\delta(\omega-\epsilon_{\mathbf{p},\sigma}+\epsilon_{\mathbf{p}-\mathbf{q},\sigma}), \tag{3.11}$$

where we have introduced an energy-conserving δ function.

In general, $W_{\sigma\sigma'}(q)$ depends on the angle θ between the incident and scattered quasiparticles. That is, by definition of q, we have $q^2 = k_{F\sigma}^2 + k_{F\sigma'}'^2 - 2k_{F\sigma}k'_{F\sigma'}\cos\theta$. In the usual manner,[9–11] we can introduce a Fourier representation: $W_{\sigma\sigma'}(\cos\theta) = \sum_{\ell=0}^\infty \alpha_\ell T_\ell(\cos\theta)W_\ell^{\sigma\sigma'}$. In the following, we shall restrict ourselves to including only the $\ell = 0$ term. Thus, in this model, we set $W_{\sigma\sigma'}(\theta) = W_0^{\sigma\sigma'}$. Then, performing the angular integration and using Eq. (3.6), we find

$$\begin{aligned}\frac{1}{\tau_{\sigma-\sigma}} = {} & W_0^{\sigma-\sigma}\left(\frac{2m^*_{-\sigma}}{h^2}\right)^2\int_{-\infty}^\infty d\omega\frac{1}{(1-e^{-\beta\omega})(1+e^{-\beta(\epsilon_{\mathbf{p},\sigma}-\mu_\sigma-\omega)})}\int_0^\infty\frac{dq}{q}\\ & \times\left\{\sqrt{\frac{\left(\frac{qp_{-\sigma}}{m^*_{-\sigma}}\right)^2-\left(\omega-\frac{q^2}{2m^*_{-\sigma}}\right)^2}{\left(\frac{qp_\sigma}{m^*_\sigma}\right)^2-\left(\omega+\frac{q^2}{2m^*_\sigma}\right)^2}}\theta\left(\frac{qp_\sigma}{m^*_\sigma}-\left|\omega+\frac{q^2}{2m^*_\sigma}\right|\right)\theta\left(\frac{qp_{-\sigma}}{m^*_{-\sigma}}-\left|\omega-\frac{q^2}{2m^*_{-\sigma}}\right|\right)\right.\\ & \left.-\sqrt{\frac{\left(\frac{qp_{-\sigma}}{m^*_{-\sigma}}\right)^2-\left(\omega+\frac{q^2}{2m^*_{-\sigma}}\right)^2}{\left(\frac{qp_\sigma}{m^*_\sigma}\right)^2-\left(\omega+\frac{q^2}{2m^*_\sigma}\right)^2}}\theta\left(\frac{qp_\sigma}{m^*_\sigma}-\left|\omega+\frac{q^2}{2m^*_\sigma}\right|\right)\theta\left(\frac{qp_{-\sigma}}{m^*_{-\sigma}}-\left|\omega+\frac{q^2}{2m^*_{-\sigma}}\right|\right)\right\}.\end{aligned} \tag{3.12}$$

The step functions determine the allowed ranges of the ω and q integrations. By inspection of (3.12), it is clear that the integrand is dominated by the $\beta\omega\to 0$ limit. For a given temperature, the important range of values is given by $\omega \ll k_BT$. In the region of degeneracy, we also have $k_BT < \{\epsilon_{F\sigma},\epsilon_{F-\sigma}\}$. Thus, we are led to the restrictions

$$\omega \ll \{\epsilon_{F\sigma},\epsilon_{F-\sigma}\}, \tag{3.13}$$

which determine the dominant contributions from the integrand in (3.12). Further, we also need to ensure that the q constraints are always real. This is accomplished by confining the ω integration to the range $|\omega| \leqslant \omega_{\max}$ where

$$\omega_{\max} = \min\left\{\frac{p_\sigma^2}{2m^*_\sigma},\frac{p^2_{-\sigma}}{2m^*_{-\sigma}}\right\}. \tag{3.14}$$

Thus, (3.12) becomes

$$\begin{aligned}\frac{1}{\tau_{\uparrow\downarrow}} = {} & W_0^{\uparrow\downarrow}\left(\frac{2m^*_\downarrow}{h^2}\right)^2\int_{-\omega_{\max}}^{\omega_{\max}}d\omega\frac{1}{(1-e^{-\beta\omega})(1+e^{-\beta(\epsilon_{\mathbf{p},\sigma}-\mu_\sigma-\omega)})}\\ & \times\left[\left\{\theta(\omega)\int_{-p_\downarrow+\sqrt{p_\downarrow^2+2m^*_\downarrow\omega}}^{p_\downarrow+\sqrt{p_\downarrow^2+2m^*_\downarrow\omega}}\frac{dq}{q}+\theta(-\omega)\int_{p_\downarrow-\sqrt{p_\downarrow^2+2m^*_\downarrow\omega}}^{p_\downarrow+\sqrt{p_\downarrow^2+2m^*_\downarrow\omega}}\frac{dq}{q}\right\}\sqrt{\frac{\left(\frac{qp_\downarrow}{m^*_\downarrow}\right)^2-\left(\omega-\frac{q^2}{2m^*_\downarrow}\right)^2}{\left(\frac{qp_\uparrow}{m^*_\uparrow}\right)^2-\left(\omega+\frac{q^2}{2m^*_\uparrow}\right)^2}}\right.\\ & \left.-\left\{\theta(\omega)\int_{p_\downarrow-\sqrt{p_\downarrow^2-2m^*_\downarrow\omega}}^{p_\downarrow+\sqrt{p_\downarrow^2-2m^*_\downarrow\omega}}\frac{dq}{q}+\theta(-\omega)\int_{-p_\downarrow+\sqrt{p_\downarrow^2-2m^*_\downarrow\omega}}^{p_\downarrow+\sqrt{p_\downarrow^2-2m^*_\downarrow\omega}}\frac{dq}{q}\right\}\sqrt{\frac{\left(\frac{qp_\downarrow}{m^*_\downarrow}\right)^2-\left(\omega+\frac{q^2}{2m^*_\downarrow}\right)^2}{\left(\frac{qp_\uparrow}{m^*_\uparrow}\right)^2-\left(\omega+\frac{q^2}{2m^*_\uparrow}\right)^2}}\right].\end{aligned} \tag{3.15}$$

From the constraint equation (3.13), we can conclude that $p_\sigma \gg \frac{m^*_\sigma \omega}{p_\sigma}$. Thus, we can expand the integration limits and the integrands in powers of $\frac{m^*_\sigma \omega}{p_\sigma}$ to find

$$\frac{1}{\tau_{\uparrow\downarrow}} = \frac{(m^*_\downarrow)^2 m^*_\uparrow W_0^{\uparrow\downarrow}}{h^4} 4 \int_0^{\omega_{\max}} d\omega \frac{\omega}{\sinh \beta\omega} \int_{\frac{m^*_\downarrow \omega}{p_\downarrow}}^{2p_\downarrow - \frac{m^*_\downarrow \omega}{p_\downarrow}} \frac{dq}{q} \frac{1}{\sqrt{(p_\uparrow^2 - q^2/4)(p_\downarrow^2 - q^2/4)}}. \tag{3.16}$$

In (3.16), we have used the low-temperature result $\mu_\sigma = \epsilon_{\mathbf{p},\sigma} + O[(T/T_{F\sigma})^2]$ to simplify the argument of the second exponential in Eq. (3.15). This is valid only to $O(T^2)$ because this is a nonideal gas. That is, at low temperature and zero polarization (for simplicity), for an interacting system one has

$$\mu(T) = \mu(0) - \left(\frac{\partial m^*}{\partial \overline{n}}\right)_T \frac{\pi}{6} \frac{1}{\hbar^2} k_B^2 T^2, \tag{3.17}$$

where $\overline{n}$ is the areal density.[21] For an ideal gas, $(\partial m^*/\partial \overline{n})_T = 0$. This is in agreement with the exact relation for the chemical potential of an ideal Fermi gas in two dimensions: $\mu(T) = k_B T \ln[\exp(\pi \overline{n} \hbar^2/m k_B T) - 1]$, where at low temperatures the finite-T corrections are exponentially small. With this change, the integrand of Eq. (3.15) becomes even in ω.

The q integration is dominated by the lower limit:

$$\int_{\frac{m^*_\downarrow \omega}{p_\downarrow}}^{2p_\downarrow - \frac{m^*_\downarrow \omega}{p_\downarrow}} \frac{dq}{q} \frac{1}{\sqrt{(p_\uparrow^2 - q^2/4)(p_\downarrow^2 - q^2/4)}} \approx \frac{1}{p_\uparrow p_\downarrow} \ln(4\epsilon_{F\downarrow}/\omega). \tag{3.18}$$

In the limit of low temperature, the leading-order term is

$$\frac{1}{\tau_{\uparrow\downarrow}} = \frac{(m^*_\downarrow)^2 m^*_\uparrow W_0^{\uparrow\downarrow}}{h^4} \frac{(k_B T)^2}{p_\uparrow p_\downarrow} \pi^2 D^{\uparrow\downarrow}(x_{\max}) \ln(\beta\epsilon_{F\downarrow}), \tag{3.19}$$

where we have used $\beta\omega_{\max} \equiv \epsilon_{F\downarrow}/k_B T \gg 1$. The quantity $1/\tau_{\downarrow\uparrow}$ can be obtained from (3.19) by flipping all of the arrows *except* that in the argument of the ln. The function $D(x_{\max})$ introduced in (3.19) is defined by

$$D^{\sigma-\sigma}(x_{\max}) \equiv \frac{4}{\pi^2} \int_0^{x_{\max}} dx \frac{x}{\sinh x}, \tag{3.20}$$

where $x_{\max} = \beta\omega_{\max}$. The integration can be done analytically, and we find

$$D^{\sigma-\sigma}(x_{\max}) = \frac{4}{\pi^2}\left[2Li_2(e^{-x_{\max}}) - \frac{1}{2}Li_2(e^{-2x_{\max}})\right], \tag{3.21}$$

where Li_2 is the dilogarithm function.[17] In the two important limits, we have $D(0) = 0$ and $D(\infty) = 1$. The σ superscripts on D reflect the implicit σ dependence in the definition of $\omega_{\max}$: Eq. (3.14). The D functions are only used to ensure the proper full-polarization limit as discussed below.

The expression for $1/\tau_{\sigma\sigma}$ follows immediately from (3.19) after noting that for the integral equivalent to (3.16) both the upper and lower limits have leading-order contributions. We find

$$\frac{1}{\tau_{\sigma\sigma}} = \frac{(m^*_\sigma)^3 W_0^{\sigma\sigma}}{h^4} \frac{(k_B T)^2}{p_\sigma^2} \frac{3\pi^2}{4} D^{\sigma\sigma} \ln(\beta\epsilon_{F\sigma}). \tag{3.22}$$

Adding (3.19) and (3.22), the quasiparticle-quasiparticle collision frequency is given by

$$\frac{1}{\tau_\sigma} = \frac{\pi^2}{h^4} m^*_\sigma \left[\frac{3}{4}\frac{(m^*_\sigma)^2}{p_\sigma^2} D^{\sigma\sigma} W_0^{\sigma\sigma} \ln(\beta\epsilon_{F\sigma}) + \frac{(m^*_{-\sigma})^2}{p_\sigma p_{-\sigma}} D^{\sigma-\sigma} W_0^{\sigma-\sigma} \ln(\beta\epsilon_{F\downarrow})\right](k_B T)^2. \tag{3.23}$$

1. Zero-polarization limit

At exactly zero polarization, it is clear from inspection of Eq. (3.1) that the two terms reduce to the same form, and that the calculation is identical to that for $\frac{1}{\tau_{\sigma\sigma}}$. Thus, the collision frequency at zero polarization is

$$\left(\frac{1}{\tau_\sigma}\right)_0 = \frac{3\pi^2}{4}\frac{(m^*)^2}{h^4}\left[\frac{1}{2}W_0^{\sigma\sigma} + W_0^{\sigma-\sigma}\right]\frac{(k_B T)^2}{\epsilon_F}\ln(\beta\epsilon_F). \tag{3.24}$$

The $D's = 1$ at zero polarization and low temperature. It should be noted that one *can not* obtain Eq. (3.24) by taking the zero-polarization limit of (3.23).

We can obtain information concerning the small polarization limit by reexamining Eq. (3.16). The integrand can be rearranged as follows:

$$\left(\frac{1}{\tau_{\sigma-\sigma}}\right)_0 \approx \frac{(m^*_{-\sigma})^2 m^*_\sigma W_0^{\sigma-\sigma}}{h^4} 2\int_0^\infty d\omega \frac{\omega}{\sinh\beta\omega} \times \frac{1}{p_{-\sigma}^2}\int_{\frac{m^*_{-\sigma}\omega}{p_{-\sigma}}}^{2p_{-\sigma} - \frac{m^*_{-\sigma}\omega}{p_{-\sigma}}} dq \left(\frac{2}{q} + \frac{1}{(2p_{-\sigma} - q)}\right) \times \sqrt{\frac{p_{-\sigma}^2 - q^2/4}{p_\sigma^2 - q^2/4}}, \tag{3.25}$$

where this form assumes $p_\sigma \geqslant p_{-\sigma}$ and we have set the upper limit of the ω integral equal to infinity. The square-root factor is regular throughout the integration region, and $2p_{-\sigma} - q$ vanishes only at the endpoint $\omega = 0$. The first term in parentheses is a maximum at the lower limit of the q integration, and the second term is a maximum at the upper limit. At exactly zero polarization, the square-root term in (3.25) is unity, and this expression is equal to the second term in Eq. (3.24). If we perform the expansions and integrations in the usual way, we find

$$\left(\frac{1}{\tau_{\sigma-\sigma}}\right)_0 \approx \frac{(m^*_{-\sigma})^2 m^*_\sigma W_0^{\sigma-\sigma}}{h^4} 2\int_0^\infty d\omega \frac{\omega}{\sinh\beta\omega}\frac{1}{p_{-\sigma}^2} \times \ln\left(\frac{2p_{-\sigma}^2}{m^*_{-\sigma}\omega}\right)\left[2 + \frac{\sqrt{m^*_{-\sigma}\omega/p_{-\sigma}^2}}{(2\mathcal{P})^{\frac{1}{2}}}\right]. \tag{3.26}$$

At this stage, we see that in order to obtain the correct zero-polarization limit, we must let $\omega \to 0$ and $\mathcal{P} \to 0$ in such a way that the second term goes to unity. Thus, as the polarization vanishes, the upper limit on the ω integration also must vanish. In our approach as described above in Sec. III A, the second term is omitted since it is not lowest order in temperature.

2. *Full-polarization limit*

In the fully polarized limit, there are no spin sums, and so the only contribution is from $\frac{1}{\tau_{\uparrow\uparrow}}$. Thus, the collision frequency at complete polarization is

$$\left(\frac{1}{\tau_\uparrow}\right)_1 = \frac{3\pi^2}{4}\frac{(m^*)^2}{h^4}\left[\frac{1}{2}W_0^{\uparrow\uparrow}\right]\frac{(k_BT)^2}{\epsilon_F}\ln(\beta\epsilon_F). \tag{3.27}$$

This result does follow from Eq. (3.23) due in part to the introduction of the D functions. This is easy to see. From the definition of the D functions (3.20), we have in the full-polarization limit ($p_\downarrow \to 0$) $D^{\uparrow\downarrow}, D^{\downarrow\uparrow}, D^{\downarrow\downarrow} \approx x_{\max} = \beta(p_\downarrow^2/2m_\downarrow^*) \ll 1$. From Eq. (3.19), we see that *without* the D function $\tau_{\sigma-\sigma}^{-1} \sim O(p_\downarrow^{-1})$. Thus, in that limit the D function drives those terms to zero. The situation is more complicated for $\tau_{\downarrow\downarrow}^{-1} \sim O(p_\downarrow^{-2})$. The D function can only cancel out the explicit $p_\downarrow$ dependence. However, from the forward scattering sum rule, we can show that $\lim_{\mathcal{P}\to 1} W_0^{\downarrow\downarrow} = 0$. From Fermi-liquid theory, we can write the transition rates in terms of the scattering amplitudes: $W_0^{\downarrow\downarrow} = \frac{2\pi}{\hbar}|a_0^{\downarrow\downarrow}|^2$. The scattering amplitudes are obtained from the Landau parameters using[9]

$$a_\ell^{\downarrow\downarrow} = \frac{f_\ell^{\downarrow\downarrow}(1+N_0^\uparrow f_\ell^{\uparrow\uparrow}) - N_0^\uparrow (f_\ell^{\downarrow\uparrow})^2}{(1+N_0^\uparrow f_\ell^{\uparrow\uparrow})(1+N_0^\downarrow f_\ell^{\downarrow\downarrow}) - N_0^\uparrow N_0^\downarrow (f_\ell^{\uparrow\downarrow})^2}, \tag{3.28}$$

where the density of states N_0^σ is defined in Eq. (2.8a). In the limit of full polarization, $f_\ell^{\uparrow\downarrow} = f_\ell^{\downarrow\downarrow} = 0$ for $\ell \geqslant 1$.[22] Thus, from (3.28), $a_\ell^{\downarrow\downarrow} = 0$ for $\ell \geqslant 1$ in the $p_\downarrow \to 0$ limit. But, the down-spin forward scattering sum rule is $\sum_{\ell=0}^\infty a_\ell^{\downarrow\downarrow} = 0$. Thus, we conclude that $a_0^{\downarrow\downarrow} = 0$.

The vanishing of $(\frac{1}{\tau_{\uparrow\downarrow}})$ and $(\frac{1}{\tau_{\downarrow\uparrow}})$ in the $p_\downarrow \to 0$ limit is due to the vanishing of the available phase space. If we assume that $p_{-\sigma}$ is the minority Fermi sea, then from Eq. (3.12) it is obvious by inspection that when $p_{-\sigma} \to 0$ one step function in each pair must vanish for all q. The situation is more complicated for $(\frac{1}{\tau_{\downarrow\downarrow}})$ since in that limit the denominator of the first square root in the curly brackets also vanishes. In this case, we proved above that $W_\ell^{\downarrow\downarrow} = \frac{2\pi}{\hbar}|a_\ell^{\downarrow\downarrow}|^2 = 0, \forall \ell$.

B. Quasiparticle-phonon collisions

By definition, an adsorbed Fermi-liquid film such as ^{3}He is in close proximity to a substrate surface, and so in principle one should also look for relaxation due to quasiparticle-phonon interactions. In fact, we shall show that for ^{3}He on a preplated ^{4}He substrate, the mismatch between the maximum Fermi velocity in the ^{3}He film and the speed of sound in the ^{4}He substrate rules out any dynamical role from the substrate. The contribution to the quasiparticle scattering rate can come from both phonon emission and absorption processes. Thus,

$$\left(\frac{1}{\tau_p}\right)_{q-p} = \frac{1}{\tau_p^{em}} + \frac{1}{\tau_p^{abs}}. \tag{3.29}$$

The two scattering rates can be written as

$$\frac{1}{\tau_p^{em}} = \frac{1}{A}\sum_{\mathbf{q}} W(q)\bar{n}_{\mathbf{p}-\mathbf{q}}[n_{ph}(q)+1]\delta(\epsilon_{\mathbf{p}} - \epsilon_{\mathbf{p}-\mathbf{q}} - \hbar\omega_q), \tag{3.30a}$$

$$\frac{1}{\tau_p^{abs}} = \frac{1}{A}\sum_{\mathbf{q}} W(q)\bar{n}_{\mathbf{p}+\mathbf{q}}n_{ph}(q)\delta(\epsilon_{\mathbf{p}+\mathbf{q}} - \epsilon_{\mathbf{p}} - \hbar\omega_q), \tag{3.30b}$$

where $\bar{n}_{\mathbf{p}}$ is defined in (3.2), $n_{ph}(q)$ is a phonon (boson) distribution function, and $\hbar\omega_q = c_s q$ is the substrate phonon spectrum. We can adapt a result of Callaway's[23] for the transition rate $W(q)/A$ in the Debye approximation

$$W(q) = \frac{\pi\hbar q_D n_4}{m_4 k_B \Theta_D} q|V(q)|^2, \tag{3.31}$$

where $V(q)$ is the Fourier transform of the lateral adatom-substrate potential, and $n_4 = N_4/L^2$ is the areal density of the ^{4}He substrate preplating.

We first examine the contribution from phonon emission. Using the techniques described above in Sec. III, we immediately find

$$\frac{1}{\tau_p^{em}} = \frac{m_3^*}{2\pi^2\hbar^2}\int_0^\infty dq \frac{W(q)}{\sinh(\beta\hbar\omega_q)} \times \frac{\theta(\epsilon_{\mathbf{p}} - \hbar\omega_q)\theta[2p - (2m_3^* c_s/\hbar + q)]}{\sqrt{4p^2 - (2m_3^* c_s/\hbar + q)^2}}, \tag{3.32}$$

where c_s is the sound speed in the substrate. The second step function imposes a constraint on the allowed range of q:

$$\hbar q < 2m_3^*(v_F - c_s). \tag{3.33}$$

The Debye temperature for the ^{4}He preplating monolayer can be taken from Hering, Van Sciver, and Vilches:[24] $\Theta_D = 26.6$ K, at a density $=0.093$ Å^{-2}, which yields a Debye wave vector $q_D = 1.081$ Å^{-1}, and a sound speed $c_s = 322$ m/s. Polarization-dependent Fermi velocities for ^{3}He films can be found in Fig. 9 of Ref. 10. At the lowest density shown (0.0132 Å^{-2}), the Fermi velocity ranges from approximately 50 m/s at zero polarization up to about 100 m/s at full polarization. At the highest density shown (0.0543 Å^{-2}), the Fermi velocity ranges from about 25 m/s at zero polarization up to about 180 m/s at full polarization. We note that much of this variation of the Fermi velocity with polarization is due to the decrease in the effective mass as a function of polarization at a fixed areal density. All of the Fermi velocities are smaller than the substrate sound speed and so the condition (3.33) is never met. Thus, the emission process is not allowed.

Using Eqs. (3.30) and (3.31), the relaxation time due to phonon absorption can be written as

$$\frac{1}{\tau_p^{abs}} = \frac{m_3^*}{2\pi^2\hbar^2}\int_{q_-}^{q_+} dq \frac{W(q)}{\sinh(\beta\hbar\omega_q)} \times \frac{1}{\sqrt{4p^2 - (2m_3^* c_s/\hbar - q)^2}}, \tag{3.34}$$

where the endpoints of the q integration are given by

$$\hbar q_{\pm} \equiv 2m_3^*(c_s \pm v_F). \tag{3.35}$$

The $q_{\pm}$ are roots of the square root in the denominator; however, the $\frac{1}{\sqrt{x}}$ type of divergence is integrable. The overwhelmingly dominant term in this expression is the argument of the sinh. The typical phonon energy is given by $\hbar\omega_q = 2m_3^*(c_s \pm v_F)c_s \sim 200$ K. Since common experimental temperatures[25] are on the order of $\beta^{-1} \sim 5$–10 mK, it is clear that for this system, phonon absorption is also frozen out because of the mismatch between accessible Fermi velocities and the substrate speed of sound.

IV. APPLICATION TO ^{3}He THIN FILMS

In this section, we shall apply the results of Secs. II and III to the thin-film Fermi-liquid system of adsorbed second-layer ^{3}He on graphite or preplated graphite. The review article by Godfrin and Lauter[7] contains a summary of the relevant experimental literature, together with a detailed description of the properties of this system. As shown above, the key elements needed to calculate the sound speeds and attenuation are the Landau parameters. In previous work,[9,10] exact analytic expressions for the Landau parameters were obtained from perturbation-theoretic calculations of the ground-state energy of a two-dimensional many-fermion system to quadratic order in the s-wave (g_0) and p-wave (g_1) effective interaction parameters. The values of these parameters were obtained by fitting existing heat-capacity effective masses reported by Greywall,[5] and spin susceptibility measurements reported by Lusher, Cowan, and Saunders.[6] An important advantage of fitting the underlying interaction parameters directly instead of the state-dependent Landau parameters is the ability to compute the angular components of the Landau parameters to all orders. In this approach, the basic assumption is that the low-density energy expression is a reasonable model at the moderate submonolayer coverages of interest. Figure 1, reproduced from Ref. 10, shows the fitted, effective s- and p-wave T-matrix components as functions of density. We note in support of our basic assumption that the parameters show only modest dependence on density.

The relations that connect the Landau parameters to the T-matrix effective interactions are lengthy, and so we refer the reader to Refs. 9 or 10 for the details. In Fig. 2, we reproduce from Ref. 10 the density and polarization dependence of the Landau parameters: $\tilde{F}_0^{\uparrow\uparrow}$, $\tilde{F}_0^{\uparrow\downarrow}$, and $\tilde{F}_0^{\downarrow\downarrow}$. These are the most important input for the sound speeds and attenuation. For a similar figure showing the $\ell = 1$ Landau parameters, see LAM. These Landau parameters are scaled with the bare, single spin-state density of states as discussed in Sec. II B.

The Landau parameters yield the zero-sound and first-sound speeds. The Fermi-liquid theory expressions for the zero-sound speeds can be found in Eqs. (2.22), (2.37), and (2.51). Similarly, the expressions for the first-sound speeds can be found in Eqs. (2.27), (2.44), and (2.56). In Fig. 3, we show the results of the calculations of the sound speeds using $\ell = 0$ and 1 Landau parameters. In Ref. 10, we showed that for accurate results one can either truncate the zero-sound speed calculation after $\ell = 1$ or 3 because of the nonmonotonicity of the Landau parameters. It should be noted that when the zero-sound calculation is carried beyond the $\ell = 1$ contribution, the resulting high-order polynomial allows multiple propagating solutions in principle. We find one and only one such solution at each density and polarization. Figure 3 shows that for a thin ^{3}He film at low coverages, the zero-sound speed is larger than the first-sound speed at a given density and polarization. It is the main objective of this work to compute the transition from one sound speed to the other as a function of temperature.

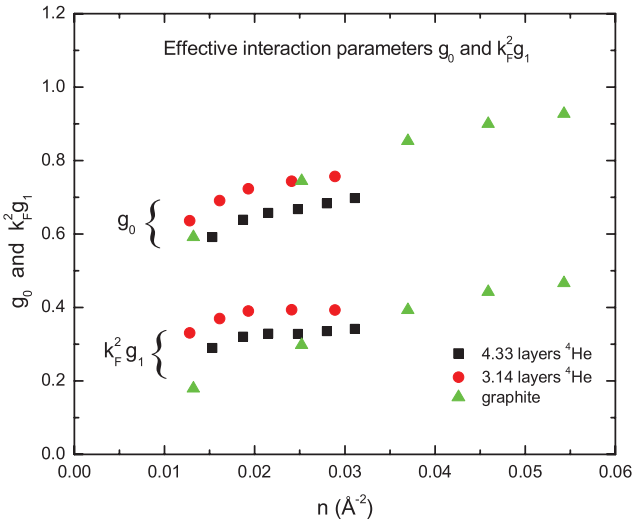

FIG. 1. (Color online) The fitted values of the effective interaction parameters g_0 and $k_F^2 g_1$ as a function of film coverage. The triangles are determined from measurements of the effective mass and spin susceptibility of second-layer ^{3}He on a graphite substrate. These are the data used in the calculations reported in this paper. The squares and circles are from ^{3}He-^{4}He thin mixture film data of Ref. 15, which are shown for comparison.

We collect in Table I the values of the zero-polarization limit, symmetric and antisymmetric, $\ell = 0$ and 1 Landau

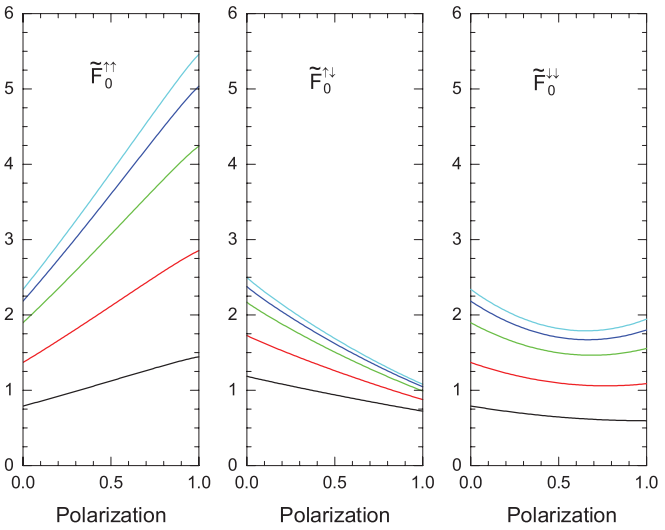

FIG. 2. (Color online) The Landau parameters $\tilde{F}_0^{\uparrow\uparrow}$, $\tilde{F}_0^{\uparrow\downarrow}$, and $\tilde{F}_0^{\downarrow\downarrow}$ for a thin ^{3}He film on graphite at five coverages as a function of polarization. In each figure, the lowest curve corresponds to the lowest coverage, and the curves progress in order up to the highest curve at the highest coverage. The five coverages are $\bar{n} = 0.0132$, 0.0252, 0.0370, 0.0459, and 0.0543 Å^{-2}.

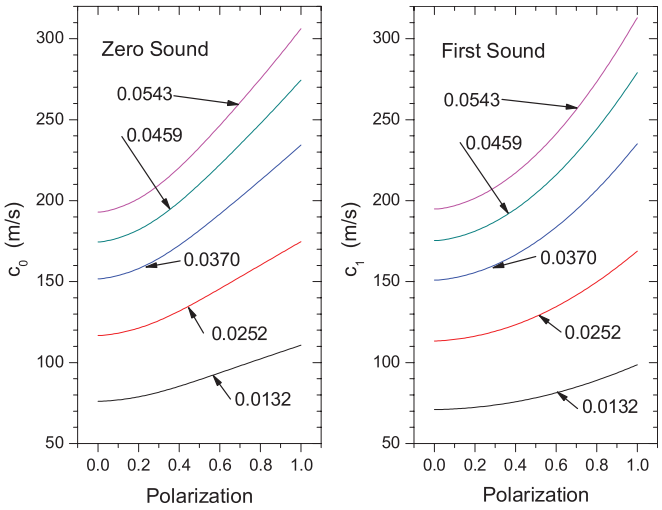

FIG. 3. (Color online) Zero-sound and first-sound speeds from Ref. 10 for ^{3}He on graphite for the five coverages $\bar{n} = 0.0132, 0.0252, 0.0370, 0.0459$, and 0.0543 Å^{-2}.

parameters. $F_0^{\rm a}$ and $F_1^{\rm s}$ are determined by fitting the spin susceptibility and the effective mass, respectively, whereas $F_0^{\rm s}$ and $F_1^{\rm a}$ are predicted values. These zero-polarization Landau parameters are normalized by the customary actual, two spin-state density of states. At zero polarization, the stability of the zero-sound mode is due to the fairly large value of F_0^s. Likewise, the instability of the spin zero-sound mode is due to the small and negative values of F_0^a. Our results indicate that at absolute zero, zero sound will propagate at all polarizations, and that spin zero sound *will not propagate* in any of these thin-film systems. At absolute zero, first sound does not propagate in a normal Fermi liquid [see, for example, Eqs. (2.28) and (3.24) at $\mathcal{P} = 0$].

As mentioned in Sec. III A2, the Landau parameters also determine the transition probabilities $W_0^{\sigma\sigma'}$'s. The transition probabilities can be expressed in terms of the scattering amplitudes: $W_0^{\sigma\sigma'} = \frac{2\pi}{\hbar}|a_0^{\sigma\sigma'}|^2$, and the scattering amplitudes can be written in terms of the Landau parameters. For $a_\ell^{\downarrow\downarrow}$, see Eq. (3.28); for $a_\ell^{\uparrow\uparrow}$, flip the spins in (3.28); and for $a_\ell^{\uparrow\downarrow}$, replace the numerator in (3.28) by $f_\ell^{\uparrow\downarrow}$. In Fig. 4, we show $|a_0^{\sigma\sigma'}|^2$ as a function of polarization at $n_3 = 0.0132$ Å^{-2}. In the $\mathcal{P} = 0.0$ limit, scattering in the antiparallel spin channel dominates, as is to be expected from Pauli principle considerations. In the limit $\mathcal{P} \to 1$, scattering in the spin parallel channel for the majority Fermi sea becomes dominant as the probability of antiparallel spin collisions goes to zero.

TABLE I. The $\ell = 0,1$ symmetric and antisymmetric Landau parameters for second-layer ^{3}He on a graphite substrate. Note that these are defined with the two spin-state density of states $F_\ell^{\rm a,s} = 2(m^*/m)\tilde{F}_\ell^{\rm a,s}$.

Density (Å^{-2})	$F_0^{\rm s}$	$F_0^{\rm a}$	$F_1^{\rm s}$	$F_1^{\rm a}$
0.013	2.56	−0.50	0.30	−0.32
0.025	5.32	−0.62	0.72	−0.56
0.037	10.7	−0.72	1.6	−0.96
0.046	16.7	−0.72	2.6	−1.3
0.054	23.6	−0.80	3.8	−1.8

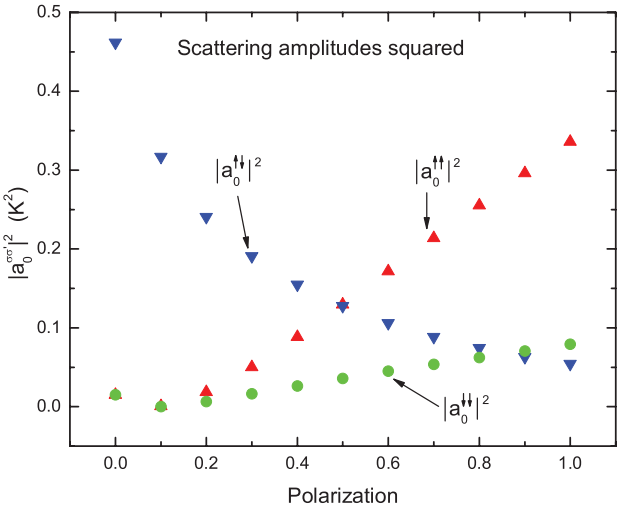

FIG. 4. (Color online) The square of the scattering amplitudes as a function of polarization at $n_3 = 0.0132$ Å^{-2}. At $\mathcal{P} = 0$, the antiparallel channel dominates. In the limit of $\mathcal{P} \approx 1$, the parallel spin channel for the majority Fermi sea dominates.

The scattering rates given by Eqs. (3.23), (3.24), and (3.27) are shown in Fig. 5 as a function of temperature at the coverage $n_3 = 0.0132$ Å^{-2}, and three polarizations $\mathcal{P} = 0, 0.5, 1$. Driven by the Pauli principle, the scattering rate is a maximum at zero polarization, and then dramatically decreases with increasing polarization. At polarizations between zero and one, the scattering rate is state dependent. In Fig. 5, one can just make out the double line at $\mathcal{P} = 0.5$ that is due to $1/\tau_\uparrow > 1/\tau_\downarrow$. The components of the scattering rates as defined by Eqs. (3.10) are shown in Fig. 6 for $\mathcal{P} = 0.5$. The figure shows that the dominant contribution to each of the scattering rates comes from the spin antiparallel channels. In addition, the scattering rates must also increase with increasing temperature as the Fermi surfaces become more diffuse. In Fig. 7, we

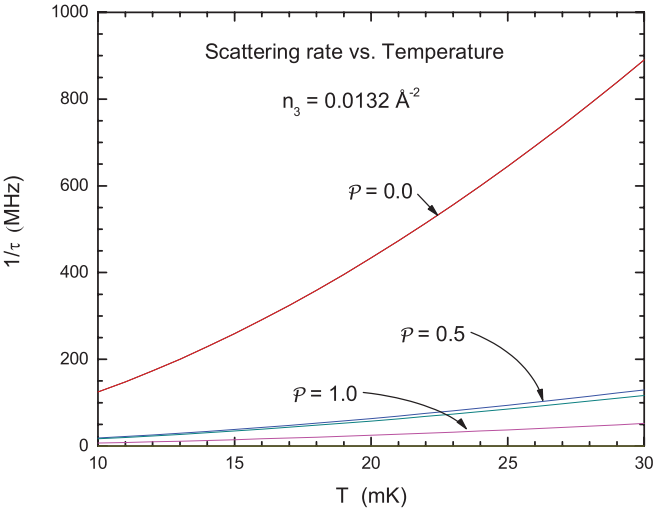

FIG. 5. (Color online) Scattering rates as a function of temperature for three polarizations $\mathcal{P} = 0, 0.5, 1.0$, and density $n_3 = 0.0132$ Å^{-2}. This figure illustrates the dramatic decrease in scattering rate as the antiparallel spin scattering channel is shut down. At $\mathcal{P} = 0.5$, the slightly higher scattering rate is $1/\tau_\uparrow$ as shown in Fig. 6.

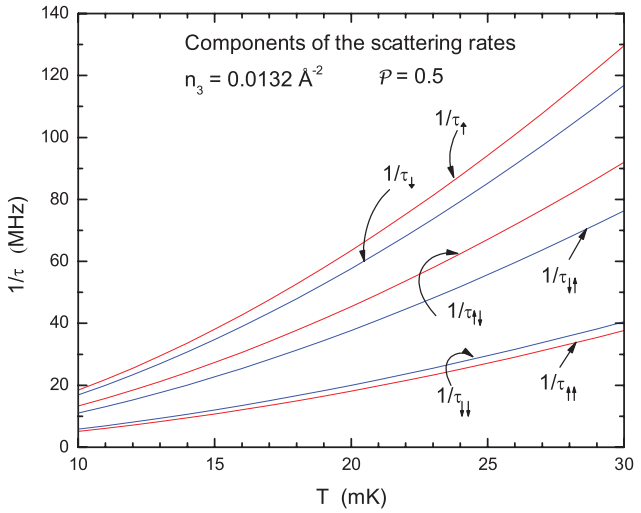

FIG. 6. (Color online) The components of the scattering rate as defined in Eq. (3.10) at $\mathcal{P} = 0.5$ and $n_3 = 0.0132$ Å^{-2}. This figure shows the dominance of scattering contributions from the antiparallel spin scattering channel for both the majority and minority constituents.

examine the polarization dependence of the scattering rates at a fixed temperature 10 mK. The majority-spin scattering rate decreases monotonically as a function of polarization due to the increasing improbability of antiparallel scattering as discussed above. On the other hand, the minority-spin scattering rate goes through a minimum around $\mathcal{P} = 0.54$ and then increases until the D function defined in Eq. (3.20) drives the scattering rate to zero in the limit of full polarization. On the right-hand ordinate of this figure, we show $T_{F\downarrow}$. The increase in the scattering rate begins at a Fermi temperature of 272 mK. At this point, the system is still deep in the low-temperature limit. This behavior is artificial, and is probably due to slightly wrong polarization dependence of the scattering amplitudes.

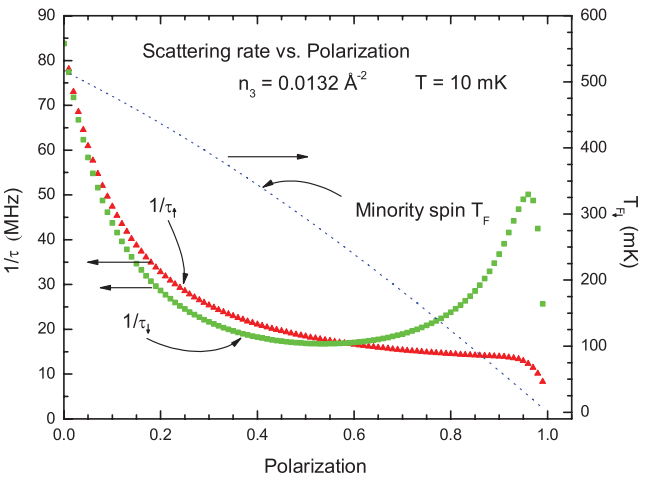

FIG. 7. (Color online) The scattering rates $1/\tau_\uparrow$ and $1/\tau_\downarrow$ as a function of polarization $\mathcal{P}$ at $T = 10$ mK, and $n_3 = 0.0132$ Å^{-2} on the left ordinate. The minority-spin Fermi temperature $T_{F\downarrow}$ vs polarization on the right ordinate (dashed line). The increase in scattering rate for the minority-spin constituent begins at $\mathcal{P} = 0.54$ where $T_{F\downarrow} = 272$ mK.

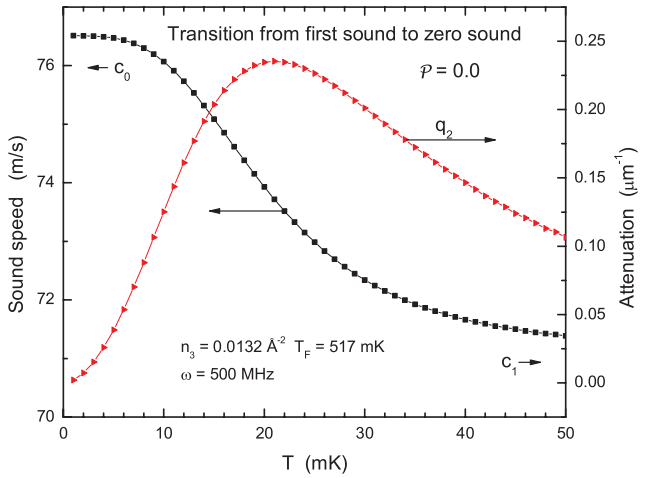

FIG. 8. (Color online) $\mathcal{P} = 0.0$ transition from first sound c_1 to zero sound c_0 as a function of temperature (left ordinate), and the attenuation q_2 as a function of temperature (right ordinate). The ^{3}He density is $n_3 = 0.0132$ Å^{-2} and the frequency $\omega = 500$ MHz. The horizontal arrows shown next to c_0 and c_1 indicate that the sound speed goes to zero sound in the low-temperature limit and first sound in the high-temperature limit.

For example, as discussed in Sec. III A2, as a consequence of the forward scattering sum rule $a_0^{\downarrow\downarrow} = 0$ in the limit of full polarization. However, in Ref. 9 it was pointed out that the scattering amplitudes derived from a low-energy expansion do not obey the forward scattering sum rules in general. The nonvanishing of $a_0^{\downarrow\downarrow}$ in the limit $\mathcal{P} = 1$ can be seen in Fig. 4. Nevertheless, in that limit there are relatively few minority spin atoms, and also $|a_0^{\uparrow\uparrow}|^2$ is approximately four times the magnitude of $|a_0^{\downarrow\downarrow}|^2$.

In Figs. 8, 9, and 10, we show the transition from first sound to zero sound with decreasing temperature at $\mathcal{P} = 0.0, 0.5, 1.0$,

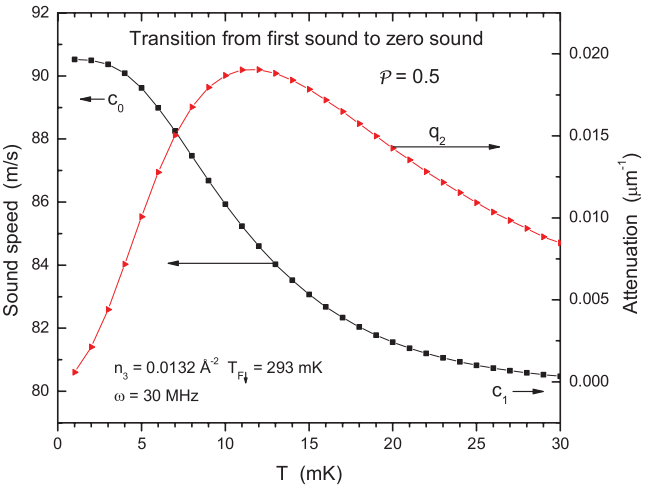

FIG. 9. (Color online) $\mathcal{P} = 0.5$ transition from first sound c_1 to zero sound c_0 as a function of temperature (left ordinate), and the attenuation q_2 as a function of temperature (right ordinate). The ^{3}He density is $n_3 = 0.0132$ Å^{-2} and the frequency $\omega = 30$ MHz. The horizontal arrows shown next to c_0 and c_1 indicate that the sound speed goes to zero sound in the low-temperature limit and first sound in the high-temperature limit.

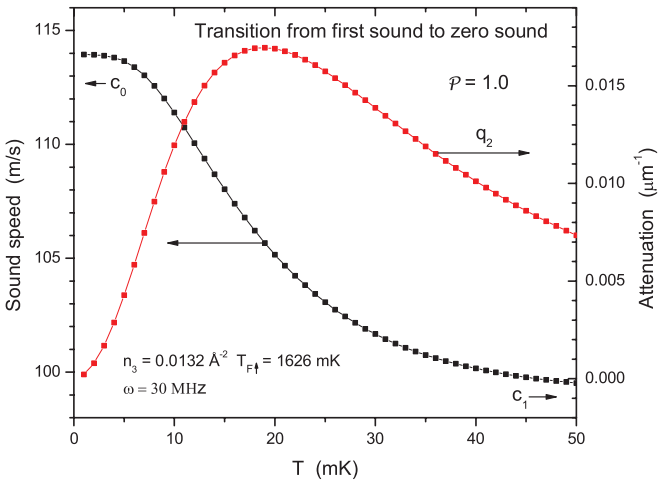

FIG. 10. (Color online) $\mathcal{P} = 1.0$ transition from first sound c_1 to zero sound c_0 as a function of temperature (left ordinate), and the attenuation q_2 as a function of temperature (right ordinate). The ^{3}He density is $n_3 = 0.0132$ Å^{-2} and the frequency $\omega = 30$ MHz. The horizontal arrows shown next to c_0 and c_1 indicate that the sound speed goes to zero sound in the low-temperature limit and first sound in the high-temperature limit.

respectively. Each of the figures is at $n_3 = 0.0132$ Å^{-2}. These results are obtained by numerically solving Eq. (2.32) for the complex q. The region of the transition is adjusted by choosing a size for the frequency ω. With larger ω, the transition moves to lower temperature. The choice is made to ensure that the transition occurs at low temperatures ($T \ll T_F$), and in an experimentally relevant interval. The need for a much larger frequency at $\mathcal{P} = 0$ than at $\mathcal{P} = 0.5$ or 1.0 can be seen directly by inspecting the scattering rates in Fig. 5. The right-hand ordinate is the attenuation q_2, the imaginary part of the wave vector. The attenuation is a maximum in the transition region where $\omega\tau \approx 1$. These figures echo the results in the classic paper of Abel, Anderson, and Wheatley[26] for bulk ^{3}He.

V. CONCLUSION

In this paper, we have studied the propagation and attenuation of zero sound and first sound in thin, arbitrarily polarized Fermi-liquid films. In Sec. II, we solved Landau's linearized kinetic equation to yield expressions for the sound speed, and also the attenuation in the relaxation-time approximation. The main results in this section for the complex speeds of sound are Eqs. (2.18) for $\mathcal{P} = 0$, (2.32) for $0 < \mathcal{P} < 1$, and (2.49) for $\mathcal{P} = 1$. In each case, the general solution was expanded in the limits $\omega\tau \gg 1$ for zero sound, and $\omega\tau \ll 1$ for first sound.

In Sec. III, we calculated the relaxation time in the low-temperature limit. We utilized an approach based on the similarity of the the collision integral to the free-fermion dynamic structure factor. The major results in this section are Eq. (3.23) for the scattering rate for $0 < \mathcal{P} < 1$, Eq. (3.24) for the scattering rate at $\mathcal{P} = 0$, and Eq. (3.27) for the scattering rate at $\mathcal{P} = 1$. We showed that the low-temperature quasiparticle-quasiparticle scattering rate $1/\tau \sim T^2 \ln(T_F/T)$. This same behavior was previously predicted to be present in the inverse spin-diffusion coefficient for two-dimensional ^{3}He by Fu and Ebner,[27] and also by Miyake and Mullin.[18]

In Sec. III B, we investigated the possibility that scattering from the substrate phonons might provide an additional limiting process for the ^{3}He quasiparticle lifetime. We showed that this was not the case. Because of the mismatch between the substrate speed of sound and the ^{3}He Fermi velocities, quasiparticle-phonon scattering was not allowed at low temperatures. This argument was made for a ^{4}He preplating substrate. We note that since the ^{4}He speed of sound is likely to be much smaller than other substrates, this result has great generality. In the absence of this result, the ^{3}He quasiparticles would *not* be infinitely long lived at absolute zero temperature.

Zero-sound propagation speeds at absolute zero temperature were discussed in our earlier publications.[9–11] Some of those results are relevant to this work. First, we note that in addition to the approach of Khalatnikov and Abrikosov,[12] which is used here to solve the linearized kinetic equation in Sec. II, there is a second approach that was introduced by Sanchez-Castro, Bedell, and Wiegers (SBW).[28] In the KA approach, one divides the kinetic equation (2.7) by the factor $(qv_F^\sigma \cos\theta - \omega)$ and then takes moments with respect to the $T_\ell(\cos\theta)$. In the SBW approach, one simply takes moments of Eq. (2.7) without dividing through by that factor. They yield different-looking expressions for the zero-sound speed; however, they are quite close numerically in the density and polarization ranges investigated in this paper. We have not applied the second approach to the kinetic equation with a collision integral. Next, we showed that truncating the kinetic equation after the $\ell = 1$ term gives results very similar to those obtained by extending the calculation to include up to $\ell = 3$. Because of the nonmonotonic behavior of the Landau parameters, one can not truncate the series after $\ell = 2$. This forms the basis for the truncation after $\ell = 1$ that is used in this work. Finally, we find one and only one propagating mode at each density and polarization. The mode is always zero sound. We do not find any values of density and polarization which admits a propagating spin-zero-sound mode. We pointed out above that this can be inferred at zero polarization from the relative values of F_0^s and F_0^a as shown in Table I. The question of whether there is a Mermin's theorem[29] at finite polarization is still being addressed.

The major results in this paper are Figs. 8, 9, and 10, showing the transition from first sound at higher temperature to zero sound at lower temperature for three polarizations: 0.0, 0.5, and 1.0, respectively. In each figure, we also include the attenuation which has a well-defined maximum (at $\omega\tau \sim 1$) in the region of the transition. We remind the reader that the transition region is tuned by adjusting the frequency. The frequencies were chosen to ensure that the transition occurred at a temperature that is small relative to the important Fermi temperatures in each case, and also was in a temperature range of interest to experiment.

Equation (2.32) is the exact solution of the linearized kinetic equation for arbitrary polarization including the $\ell = 0$ and 1 contributions. In the zero-polarization limit, it reduces to Eq. (2.34), and in the complete-polarization limit, it reduces to Eq. (2.49). By examining the solutions in the $\omega\tau \gg 1$ and $\omega\tau \ll 1$, we obtained exact, analytic expressions for the speeds

and attenuation of zero sound and first sound, respectively, for arbitrary polarization. Although, in some cases, the relations are implicit.

We found that the approach we used to compute the scattering rates due to quasiparticle-quasiparticle collisions did not permit us to obtain a single general result valid at all polarizations. Thus, the lifetime is given by three expressions valid at zero polarization, complete polarization, and at arbitrary polarizations with $\mathcal{P} \neq 0,1$. Further, the lifetime results are only valid in the limit of $T \ll T_{F\sigma}$ since they use Stern's zero-temperature result for the imaginary part of the dynamic susceptibility $\chi''(k,\omega)$ [Eq. (3.8)].[20] The limit of zero polarization is especially complicated. The limits on the q integration (3.12) can become ambiguous due to the interaction between the step-function constraints and the ω frequency integral. In the full-polarization limit, the minority Fermi sea eventually disobeys the low-temperature constraint $T \ll T_{F\downarrow}$. A fix for this situation was the introduction of the D functions in Eq. (3.20). The upper limit of the integral defining this function was chosen to be $x_{\max} = \beta\omega_{\max}$ in order to satisfy the reality constraint (3.14). We note, however, that ω should also obey the inequality Eq. (3.13), which implies that the upper limit on the D functions ought to be considerably smaller. A smaller upper limit to the integral would presumably remove the peak at high polarization shown for $1/\tau_{\downarrow}$ in Fig. 7.

The numerical results are all predictions for thin-film ^{3}He with arbitrary polarization. Testing these predictions will be difficult since polarizing the ^{3}He system means ordering a *nuclear* moment. In Ref. 10, we pointed out that there exists a single measurement of a zero-sound speed for a ^{3}He film at zero polarization by Godfrin, Meschke, Lauter, Böhm, Krotscheck, and Panholzer.[25] Their substrate was graphite, the ^{3}He areal density was $\overline{n} = 0.049$ Å^{-2}, the wave vector was $q = 5.5$ nm^{-1}, and the energy transfer was $\omega = 0.68 \pm 0.05$ meV. This yields a zero-sound speed of $c_0 \approx 190 \pm 14$ m/s. Our predicted results for this system of $c_0 = 181$ m/s are in excellent agreement. However, for the ultracold gases, nonzero polarization is not a critical issue. There has been considerable recent progress in preparing ultracold Fermi-gas systems in quasi-two-dimensional configurations. In a recent paper, Vogt, Feld, Fröhlich, Pertot, Koschorreck, and Köhl[30] report measurements of the transition between the ballistic regime to the hydrodynamic regime for a quadrupolar collective excitation in the trapped gas. They also report measurements of the shear viscosity as a function of interaction strength.

*zhaozhe.li@email.wsu.edu
†rha@spu.edu
‡mdm@wsu.edu

[1] L. D. Landau, Zh. Eskp. Teor. Fiz. **30**, 1058 (1956) [Sov. Phys.–JETP **3**, 920 (1957)]; **32**, 59 (1957) [**5**, 101 (1957)].
[2] L. D. Landau, Zh. Eskp. Teor. Fiz. **35**, 97 (1958) [Sov. Phys.–JETP **8**, 70 (1959)].
[3] J. G. Dash, *Films on Solid Surfaces* (Academic, New York, 1975).
[4] M. Bretz, J. G. Dash, D. C. Hickernell, E. O. McLean, and O. E. Vilches, Phys. Rev. A **8**, 1589 (1973); D. C. Hickernell, E. O. McLean, and O. E. Vilches, Phys. Rev. Lett. **28**, 789 (1972); S. W. Van Sciver and O. E. Vilches, Phys. Rev. B **18**, 285 (1978).
[5] D. S. Greywall, Phys. Rev. B **41**, 1842 (1990).
[6] C. P. Lusher, B. P. Cowan, and J. Saunders, Phys. Rev. Lett. **67**, 2497 (1991); M. Dann, J. Nyéki, B. P. Cowan, and J. Saunders, *ibid.* **82**, 4030 (1999).
[7] H. Godfrin and H.-J. Lauter, in *Progress in Low Temperature Physics*, Vol. XIV, edited by W. P. Halperin (Elsevier, Amsterdam, 1995), Chap. 4.
[8] R. B. Hallock, in *Progress in Low Temperature Physics*, Vol. XIV, edited by W. P. Halperin (Elsevier, Amsterdam, 1995), Chap. 5.
[9] R. H. Anderson and M. D. Miller, Phys. Rev. B **84**, 024504 (2011).
[10] D. Z. Li, R. H. Anderson, and M. D. Miller, Phys. Rev. B **85**, 224511 (2012).
[11] R. H. Anderson, D. Z. Li, and M. D. Miller, J. Low Temp. Phys. **169**, 291 (2012).
[12] I. M. Khalatnikov and A. A. Abrikosov, Zh. Eskp. Teor. Fiz. **33**, 110 (1957) [Sov. Phys.–JETP **6**, 84 (1958)]; A. A. Abrikosov and I. M. Khalatnikov, Rep. Prog. Phys. **22**, 329 (1959).
[13] J. R. Engelbrecht, M. Randeria, and L. Zhang, Phys. Rev. B **45**, 10135 (1992).
[14] K. S. Bedell and K. F. Quader, Phys. Lett. A **96**, 91 (1983); K. F. Quader and K. S. Bedell, J. Low Temp. Phys. **58**, 89 (1985).
[15] H. Akimoto, J. D. Cummings, and R. B. Hallock, Phys. Rev. B **73**, 012507 (2006); J. Cummings, H. Akimoto, and R. B. Hallock, J. Low Temp. Phys. **138**, 325 (2005).
[16] G. Baym and C. Pethick, *Landau Fermi-Liquid Theory* (Wiley, New York, 1991).
[17] *Handbook of Mathematical Functions with Formulas, Graphs, and Mathematical Tables*, edited by M. Abramowitz and I. A. Stegun (Dover, New York, 1965).
[18] K. Miyake and W. J. Mullin, Phys. Rev. Lett. **50**, 197 (1983).
[19] G. F. Giuliani and J. J. Quinn, Phys. Rev. B **26**, 4421 (1982).
[20] F. Stern, Phys. Rev. Lett. **18**, 546 (1967).
[21] A derivation of this expression for a bulk Fermi liquid can be found in Ref. 16, pp. 10 and 11.
[22] K. S. Bedell, in *Proceedings of the Third International Conference on Recent Progress in Many Body Theories*, Lecture Notes in Physics, Vol. 198, edited by H. Kümmel and M. L. Ristig (Springer, New York, 1984), pp. 200–209.
[23] J. Callaway, *Quantum Theory of the Solid State*, 2nd ed. (Academic, Boston, 1991) Chap. 7.
[24] S. V. Hering, S. W. Sciver, and O. E. Vilches, J. Low Temp. Phys. **25**, 793 (1976).
[25] H. Godfrin, M. Meschke, H.-J. Lauter, H. Böhm, E. Krotscheck, and M. Panholzer, J. Low Temp. Phys. **158**, 147 (2010).
[26] W. R. Abel, A. C. Anderson, and J. C. Wheatley, Phys. Rev. Lett. **17**, 74 (1966).
[27] H.-H. Fu and C. Ebner, Phys. Rev. A **10**, 338 (1974).
[28] C. R. Sanchez-Castro, K. S. Bedell, and S. A. J. Wiegers, Phys. Rev. B **40**, 437 (1989).
[29] N. D. Mermin, Phys. Rev. **159**, 161 (1967).
[30] E. Vogt, M. Feld, B. Fröhlich, D. Pertot, M. Koschorreck, and M. Köhl, Phys. Rev. Lett. **108**, 070404 (2012).